Stockholm University

NMR studies on interactions between the amyloid β peptide and selected molecules

Anna Wahlström

Cover illustration:
^{1}H-^{15}N HSQC spectrum of 75 μM ^{15}N-labeled Aβ(1-40)
in 10 mM sodium phosphate buffer at pH 7.4 and 5 °C.

ISBN 978-91-7447-325-4 Pages 1-59

Printed in Sweden by Universitetsservice AB, Stockholm 2011
Distributor: Department of Biochemistry and Biophysics, Stockholm University

Till Mamma, Pappa,
Sofia och Marcus

Abstract

Alzheimer's disease is an incurable neurodegenerative disorder linked to the amyloid β (Aβ) peptide, a 38-43 residue peptide. The detailed molecular disease mechanism(s) is (are) unknown, but oligomeric Aβ structures are proposed to be involved.

In common for the papers in this thesis is interactions; interactions between Aβ(1-40) and selected molecules and metal ions. The purpose has been to find out more about the structural states that Aβ can adopt, in particular the β-sheet state, which probably is linked to the oligomeric structures. The methods used have been nuclear magnetic resonance (NMR), circular dichroism (CD) and fluorescence spectroscopy using Thioflavin T (ThT).

Upon addition of SDS/LiDS detergent or Congo red (CR) to Aβ(1-40), the initial random coil/PII-helix state was transformed into β-sheet and, in the case of detergent, a final α-helical state. In contrast to SDS/LiDS and CR, the dimeric Affibody molecule locks monomeric Aβ(1-40) in a β-hairpin state. It was found that by truncating the flexible N-terminal end of the Affibody molecule its affinity to Aβ was improved. The aggregation of Aβ(1-40) was further studied in the presence of a β-cyclodextrin dimer by a kinetic assay using ThT. Although having a weak dissociation constant in the millimolar range, the β-cyclodextrin dimer modified the aggregation pathways of Aβ.

Finally Aβ(1-40) was studied in presence of Cu^{2+} and Zn^{2+} at physiological and low pH. Cu^{2+} was observed to maintain its specific binding to Aβ when decreasing the pH to 5.5 while Zn^{2+} behaved differently. This could be of importance in the Alzheimer's disease brain in which the environment can become acidic due to inflammation.

In conclusion the results show that Aβ(1-40) is very sensitive to its environment, responding by adopting different conformations and aggregating in aqueous solutions. The β-sheet state is induced by varying molecules with different properties, properties that govern the final Aβ state.

List of publications

I **Wahlström A***, Hugonin L*, Perálvarez-Marín A*, Jarvet J, Gräslund A (2008) Secondary structure conversions of Alzheimer's Aβ(1-40) peptide induced by membrane-mimicking detergents. *FEBS J 275*, 5117-5128

II Lendel C, Bolognesi B, **Wahlström A**, Dobson CM, Gräslund A (2010) Detergent-like interaction of Congo red with the amyloid β peptide. *Biochemistry 49*, 1358-1360

III Lindgren J, **Wahlström A**, Danielsson J, Markova N, Ekblad C, Gräslund A, Abrahmsén L, Karlström AE, Wärmländer SK (2010) N-terminal engineering of amyloid-β-binding Affibody molecules yields improved chemical synthesis and higher binding affinity. *Protein Sci 19*, 2319-2329

IV **Wahlström A**, Cukalevski R, Danielsson J, Jarvet J, Onagi H, Rebek J Jr, Linse S, Gräslund A. Specific binding of an engineered β-cyclodextrin dimer to the amyloid β peptide modulates the peptide aggregation process. *Manuscript.*

V Ghalebani L, **Wahlström A**, Danielsson J, Wärmländer KTS, Gräslund A. pH dependence of the specific binding of Cu(II) and Zn(II) ions to the amyloid β peptide. *Manuscript*.

* These authors have contributed equally.

Related publication not included in the thesis:

Löfgren K, **Wahlström A**, Lundberg P, Langel U, Gräslund A, Bedecs K (2008) Antiprion properties of prion protein-derived cell-penetrating peptides. *FASEB J 22*, 2177-2184

Abbreviations

Aβ	Amyloid beta
ADDL	Aβ-derived diffusible ligand
APP	Amyloid precursor protein
CD	Circular dichroism
CMC	Critical micelle concentration
CR	Congo red
FTIR	Fourier transform infrared spectroscopy
HSQC	Heteronuclear single-quantum correlation
LiDS	Lithium dodecyl sulfate
NMR	Nuclear magnetic resonance
PII helix	Polyproline II helix
ROS	Reactive oxygen species
SDS	Sodium dodecyl sulfate
ThT	Thioflavin T
TROSY	Transverse relaxation optimized spectroscopy

Contents

1. Introduction

Alzheimer's disease belongs to the group of protein misfolding diseases that encompasses about 40 different diseases. Common to all of them is that a peptide or a protein has lost its native state and is assembled in insoluble amyloid fibrils, structures that have a thread-like appearance (1). In the case of Alzheimer's disease the amyloid fibrils are found in the brain, causing neurodegeneration, but other diseases involve aggregation in tissues apart from the brain (2).

A characteristic property of the amyloid fibrils is the cross-β conformation, i.e. the β-strands making up the fibrils are oriented transversely to the axis of the fibril (fig. 1), protease resistance and binding to the dyes Congo red (CR) and Thioflavin T (ThT) (3, 4).

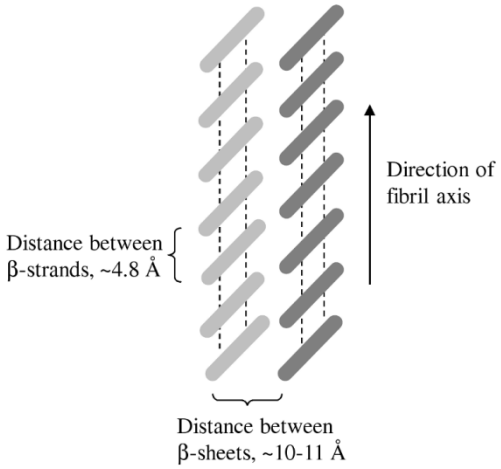

Figure 1. Schematic overview of cross-β structure in the amyloid fibril (after (3)). The individual β-strands, making up a β-sheet, are perpendicular to the fibril axis (3, 5).

1.1 Alzheimer's disease

Alzheimer's disease is named after Alois Alzheimer (1864-1915), a German professor in psychiatry. In 1906 he presented the observations that were going to link his name with the disease; neuronal loss, amyloid plaques and neurofibrillary tangles. The patient, a 51 year old woman, had started to behave differently. Her condition worsened by time, she lost her memory, got paranoid, turned disoriented and finally reached a state of apathy before she died, five years after the symptoms first appeared (6). Today Alzheimer's disease is the main cause of dementia in elderly people (7).

Dementia constitutes a group of symptoms caused by conditions that step by step destroy neurons and results in reduced mental function (8, 9). There is still no way to cure the disease, even though there are different drugs to relieve the symptoms. The life span after diagnosis is an average of four to six years, but by then the disease can have been evolving for already 14-16 years. Sometimes the progress is especially aggressive, resulting in a very short time period of about three years from outbreak to death (10).

Worldwide more than 20 million people suffer from Alzheimer's disease (11). In Sweden about 160 000 people have dementia and patients with Alzheimer's disease constitute about 60% of the cases (12). The most serious risk factor for developing the disease is age and the typical patient is 65 years or older. Above 65, the risk increases twofold every fifth year, reaching a 50% risk at an age above 85 years (10). Since the population grows older and older, Alzheimer's disease is an increasing problem in the society, both socially and economically. For example, in the USA, the prognosis is that by 2050 there will be one million new cases every year (10).

Most cases of Alzheimer's disease are sporadic, however, there is also a familial form caused by various mutations. The familiar form is rarer, but the patients are younger. The onset is before an age of 65 and sometimes there are patients as young as 40 years (13).

The signs of neurodegeneration linked to Alzheimer's disease (and also in other dementias) are first seen in the medial temporal lobe, including the hippocampus and the entorhinal cortex. This loss, or atrophy, can be seen by computed tomography (CT) and magnetic resonance imaging (MRI) (14).

As mentioned, amyloid plaques and neurofibrillary tangles are typical structures in cerebral cortex that are linked to the disease (9). Tangles are twisted strands of a distorted phosphorylated form of the neuronal microtubule-associated protein tau found inside nerve cells (15). The extracellular plaques on the other hand are associated with the amyloid β (Aβ) peptide, a

small part of a larger protein. The plaques can be visualized post-mortem by different staining techniques like antibodies and CR (16, 17).

There are different types of plaques in terms of morphology and ability to be stained and moreover the terminology varies, but commonly the plaques are referred to as being diffuse or neuritic (18). Diffuse plaques comprise structures that are quite heterogeneous and without a clear boundary. By light microscopy they are seen varying from 50 to several hundred micrometers in diameter, but electron microscopy visualizes much smaller ones as well. This type of plaque is not very immunoreactive and is seen also in individuals without clinical signs of Alzheimer's disease, which raises the question that there may exist plaques connected to ageing (16, 17, 18). The neuritic plaques are more dense and spherical and have an insoluble and fibrous core of amyloid material (19).

In the vicinity of the plaques, predominantly the neuritic ones, dystrophic neurites, i.e. abnormal axons or dendrites, are seen, as well as microglia and astrocytes. The presence of microglia and astrocytes is a sign of inflammation in the tissue (16, 18).

The component in the plaques that is subject to lots of research and is believed to be one major underlying reason for the disease is the 4.2 kDa Aβ peptide (19, 20). Other plaque components are proteins like complement factors that are part of the immune system, serum amyloid P component, apolipoproteins E and J and heparan sulfate proteoglycans (21). Also metal ions like zinc, copper and iron are found (22).

1.2 The amyloid precursor protein and the amyloid β peptide

The origin of Aβ is the amyloid precursor protein (APP), an integral receptor-like membrane protein whose gene is located on chromosome 21 (23). The main part of the protein is localized outside the cell while only a small fraction protrudes into the cell interior (24), the membrane spanning part in between is predicted to adopt α-helical structure (25). Varying cell types express APP, both neuronal and nonneuronal throughout the body (26, 27). The three major isoforms of the protein, consisting of 695, 751 and 770 amino acids, respectively, differ somewhat in their expression pattern. The shortest form is most abundant in neuronal cells and is more rare in other parts of the body while the two longer forms are more commonly found in nonneuronal than neuronal cells (27). Besides the variation in the number of amino acids, the protein also shows variability in glycosylation, sulfation and phosphorylation resulting in a size span of 110-140 kDa (26, 27) (fig. 2).

Aβ peptides are derived from APP through proteolytic processing that takes place during normal cellular metabolism (28, 29). The peptides are found in both cerebrospinal fluid and blood plasma in healthy people (29, 30). Due to the activity of different proteases the outcome of the cleavage varies. The non-amyloidogenic pathway involves cleavage of APP by α-secretase, which results in a free soluble N-terminal part (sAPPα) and a membrane-bound C-terminal region (CTF83), which is further cleaved (14, 26, 31, 32). The amyloidogenic pathway starts with the activity of β-secretase, most often represented by β-site APP cleaving enzyme 1 (BACE1), resulting in soluble sAPPβ and the C-terminal region (CTF99) attached to the membrane (33). In the next step γ-secretase, a complex consisting of at least four different proteins (presenilin 1 or 2 is one of them), cleaves CTF99 in the region going through the cell membrane (34). The resulting fragments are Aβ and the APP intracellular domain (AICD) (32) (fig. 2).

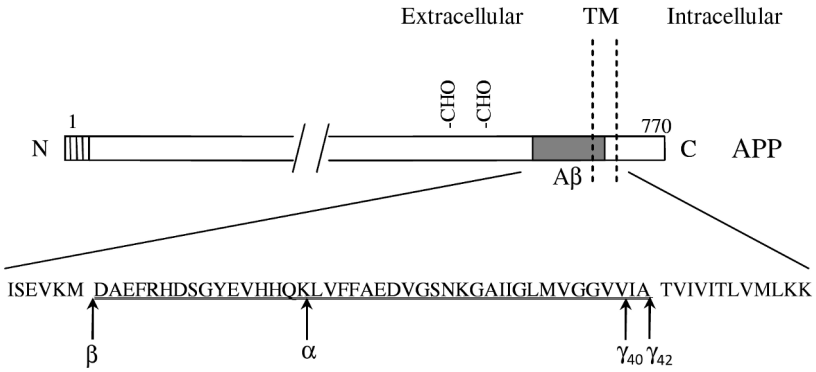

Figure 2. The amyloid precursor protein (APP) and the Aβ peptide (underlined residues). The dashed lines indicate the transmembrane (TM) part of APP. –CHO indicates a glycosylation site (23, 26). Aβ is produced by the activity of β- and γ-secretase while α-secretase leads the process into the non-amyloidogenic pathway (14, 33, 34).

Both β- and γ-secretase have more than one cleavage site resulting in Aβ peptide heterogeneity (15). Aβ(1-40) and Aβ(1-42) are the most frequently occurring peptides, consisting of 28 residues of the extracellular domain of APP and 12 and 14 residues of the transmembrane domain, respectively. However, there are peptides in the span from Aβ(1-37) to Aβ(1-43), and also N-terminal truncated forms like Aβ(11-40) exist (20, 23, 35). Aβ(1-40) is the dominating species in the extracellular fluid or cerebrospinal fluid, yet Aβ(1-42) is the major component in senile plaques (36, 37, 38).

Aβ(1-40) is an amphiphilic peptide with a charged and relatively hydrophilic N-terminal part, a central hydrophobic segment and a hydrophobic C-terminus (fig. 3). At physiological pH, about 7.4, the peptide has a net charge of -3. The histidines are sensitive to pH changes, but at physiological pH they are uncharged. The hydrophobic parts of Aβ are important for its aggregation propensity (39). This is especially seen for Aβ(1-42) that has two additional hydrophobic amino acids in the C-terminus and therefore is much more prone to aggregate (40).

Figure 3. The amino acid sequence of Aβ(1-40) with charges at physiological pH. Red letters: acidic negatively charged residues, blue letters: basic positively charged residues, green letters: polar uncharged residues, black letters: nonpolar residues. Histidines (H), uncharged at physiological pH and positively charged below pH ~6, are indicated by purple letters.

Despite intense research on the biological functions of APP, nothing definite is known. There are however several processes to which APP and/or its various fragments have been linked; adhesion (to other cells or to the extracellular matrix), signaling, neurite outgrowth regulation, calcium homeostasis, cell survival and cell death (24). Further, APP has zinc and copper metal binding sites and has been suggested to be important for homeostasis of metals (41, 42).

1.3 The amyloid cascade hypothesis

In 1992 the amyloid cascade hypothesis was presented (20), which states that the Aβ peptide and its accumulation in plaques is the first step towards Alzheimer's disease and that genetic factors predispose the peptide production. The other characteristics of the disease; neurofibrillary tangles, neuronal death and memory impairment are secondary effects of the Aβ plaque formation (20). However, one important observation that challenges the hypothesis is that the degree of dementia does not clearly correlate with the amyloid plaque load, but rather with the concentration of soluble peptide (43). Other weaknesses of the hypothesis concern the postulated connection between Aβ and formation of neurofibrillary tangles and the issue of what actually comes first - plaques and tangles formation or neurodegeneration (44)?

1.4 The Aβ aggregation process

The aggregation process of Aβ, described as a nucleation-dependent polymerization, starts with unstructured Aβ peptides that are converted into intermediate states containing some degree of β-sheet structure. Assembly of these intermediates, which are "supersaturated" in the solution, into a nucleus results in stabilization. After the nucleation phase, also called the lag phase, the elongation phase starts with the formation of oligomers and higher order aggregates, also called protofibrils. In the final steady state phase, fibrils in equilibrium with monomers are found (fig. 4) (19, 45, 46). Traditionally the aggregation process has been considered to be governed by the nucleation events, however, already formed larger structures can split and form fragments. This filament fragmentation process is a secondary nucleation mechanism that contributes to the kinetics of aggregation (47).

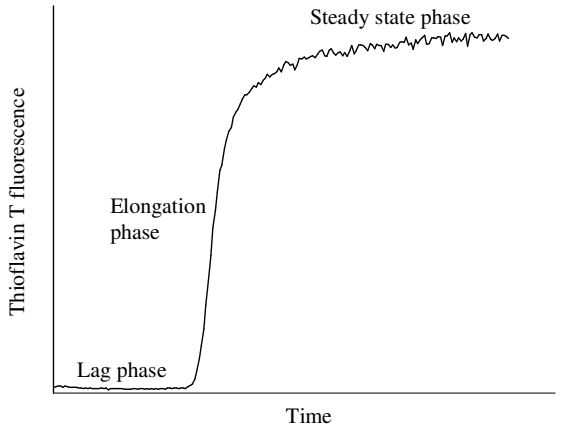

Figure 4. An example of the characteristic sigmoidal curve describing the aggregation process of the Aβ peptide. The process is initiated by the slow lag phase in which nuclei of peptide are formed that during the elongation phase assemble and grow rapidly by primary and secondary nucleation events (46, 47). Mature fibrils that are in equilibrium with monomeric peptide are found in the steady state phase (46). The aggregation in this example is measured by recording fluorescence from Thioflavin T that binds to β-sheet structures (48).

Many factors have been found to influence the Aβ fibrillation process, for example the initial peptide aggregation state, peptide concentration, peptide length and amino acid substitutions, temperature, pH and interaction with different types of molecules (49, 50). In addition, metal ions like Zn^{2+}, Fe^{3+} and Cu^{2+} have been proposed to have an impact on the aggregation process and the precipitation of amyloid fibrils (49).

1.5 Amyloid structure

In 2004 the following was stated about amyloid structure: "extracellular depositions of protein fibrils with characteristic appearance in electron microscope, typical X-ray diffraction pattern, and affinity for Congo red with concomitant green birefringence" (51). Furthermore, the deposits have a fibrillar appearance and the X-ray diffraction pattern indicates cross-β sheet (21).

The terminology is however not completely clear. The definition above concerns amyloid fibrils that are found naturally and extracellularly in body tissues, always associated with the serum amyloid P component and proteoglycans (51). However, from a structural point of view, peptides of various kinds can *in vitro* adopt cross-β structure and subsequently bind to CR, stretching the definition of amyloid. This also implicates that amyloid formation is not a result of a specific amino acid sequence, but is rather a property of the polypeptide chain (3). This leads to the alternative definition of amyloid fibrils as "fibrillar polypeptide aggregates with cross-β conformation" (3). An example of this is the sequence GNNQQNY from the yeast protein Sup35. This short sequence forms amyloid-like fibrils that fulfill all the requirements for being an amyloid structure. At millimolar concentration it forms microcrystals suited for X-ray diffraction experiments, revealing an atomic model of the spine of the amyloid structure (52). The peptide is arranged in parallel and in-register β-strands that form the β-sheet. Two β-sheets are then associated; the β-strands in one sheet are antiparallel to the ones in the other sheet and moreover the β-sheets are somewhat dislocated to each other making it possible for the side chains to wedge and form a "steric zipper" (52).

For insoluble fibrils it is impossible to use solution state nuclear magnetic resonance (NMR) spectroscopy for characterization. Useful methods are for example electron and atomic force microscopy, infrared (IR) spectroscopy and, as already mentioned, X-ray diffraction (5). Another alternative to identify amyloid structure is to use dyes and ThT is very common in this context in addition to CR. There are however difficulties with these dyes since it is not clarified in detail to what structure these dyes actually bind.

1.5.1 Congo red birefringence

CR is a histological dye that binds to β-sheet structure and visualizes amyloid material by showing green birefringence (53). It has both hydrophobic and hydrophilic character; the two phenyl rings in the centre each links to a naphthalene group with a sulfonic acid and an amine group (fig. 5). At physiological pH the two sulfonic acid groups are negatively charged (54).

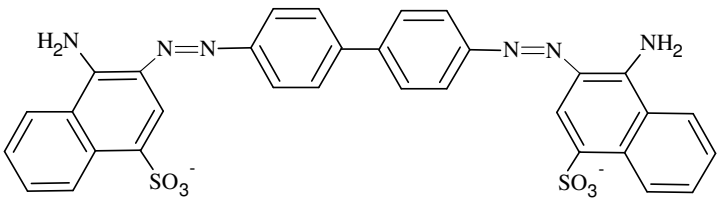

Figure 5. Chemical structure of Congo red.

The binding mechanism for CR to amyloid is not completely known but there are various binding models. One of them gives two possible explanations for the binding of CR to amyloid material; β-sheet structure and positive charge. The β-sheet structure implies that β-strands are packed side by side with a repetitive occurrence of a positively charged N-terminus. This nicely fits with the binding of a CR molecule that has one negative charge at each end, matching every fifth positive N-terminus (55).

Another binding model involving insulin instead proposes that CR is inserted between the antiparallel β-strands making up the amyloid structure (56). However, although β-sheet structure binds CR, it is not the sole prerequisite for binding since α-helices also have been shown to bind the dye (55).

An additional explanation for the amyloid staining ability of CR is its property of assembling into micelles. The micelles expose hydrophobic regions that could interact with the polypeptide backbone (57).

1.5.2 Thioflavin T fluorescence

ThT is a very common marker for probing the presence of amyloid material that is formed by different proteins and peptides like for example Aβ, insulin, lysozyme and α-synuclein. When this cationic benzothiazole dye (fig. 6) binds to amyloid structures an extra absorption peak at 450 nm appear in the excitation spectrum and an enhanced fluorescence is observed at an emission wavelength of 480 nm (58, 59, 60).

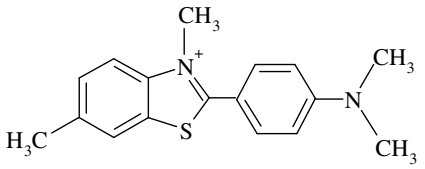

Figure 6. Chemical structure of Thioflavin T.

The ThT binding mechanism to amyloid structure is not known in detail, but the presence of cross-β structure seems crucial (61). The proposed suggestions on the detailed structures of the complexes formed and on the induced fluorescence of the ThT in the complex are variable. One of them, the "channel model", states that ThT is positioned within the channel that is formed by the side-chains in the cross-β structure and that the long axis of the molecule is parallel to the long axis of the fibril (62). The increased fluorescence upon binding has been proposed to occur because the two halves of the molecule become rigid relative to one another, thereby avoiding quenching (63).

Another model is based on the amphiphilicity of ThT with the hydrophobic phenyl group linked to a dimethylamino group and the more polar part, the benzothiazole group (fig. 6). This would drive the formation of micelles that could interact hydrophobically with the grooves of the amyloid structures (58).

Aromatic amino acid residues have been found to be beneficial for ThT binding while charged residues can have the opposite effect. This is exemplified by a positively charged fibril forming peptide, with amino acid sequence KLKLKLELELELG, which does not cause enhanced ThT fluorescence (58, 61). These findings imply that the binding of ThT might not be exclusively dependent on β-sheet structure but that there may be an ionic contribution as well (58).

A third alternative under debate is that ThT might bind fibrils as a dimer forming an excimer (64).

1.6 Oligomers

During many years the insoluble Aβ fibril was considered as the toxic entity causing Alzheimer's disease (65, 66, 67). But in fact the connection between the severity of the disease and the presence of Aβ plaques is not clear-cut (68). An example of this is that Aβ deposition in the brain, unrecognizable from the one found in patients with Alzheimer's disease, has been observed postmortem in older individuals that did not display any signs of the disease (69, 70). Furthermore, in mice it has been seen that amyloid plaque formation is preceded by reduced density of presynaptic terminals and neurons along with impaired synaptic transmission (71).

Instead, the levels of soluble Aβ in the brain have been found to correlate better with synapse loss and Alzheimer's disease; higher levels are a stronger indication of dementia (69, 72, 73). Soluble Aβ can be monomeric but also aggregated in the form of various assemblies, widely spoken of as oli-

gomers (73). The oligomers are suggested to assemble by hydrogen bonds resistant to sodium dodecyl sulfate (SDS) and urea, but sensitive to hexafluoroisopropanol (HFIP) (74).

Studies with synthetic Aβ peptides indicate that freshly made, soluble Aβ monomer is rather inert and that the toxicity rather is derived from the aggregated, oligomeric and polymeric Aβ forms (75). Oligomers are defined as soluble if they remain in the aqueous supernatant after centrifugation at 220,000 × g for 2 hours. Ultrafiltration following this centrifugation has revealed the size intervals >100 kDa, 30-100 kDa, 10-30 kDa and <10 kDa of smaller and larger oligomers (73). Aβ has been observed in many different kinds of assemblies, both *in vivo* and as a synthetic peptide *in vitro* and its widely varying appearance can probably partly be explained by different preparation protocols and analysis techniques.

Reported oligomeric terms, with more or less overlapping definitions, in the literature are protofibrils, annular assemblies, Aβ-derived diffusible ligands (ADDLs), Aβ*56 and dimers and trimers (76). The term protofibril is used for an intermediate state in the aggregation process, observed for synthetic Aβ. The state is characterized by short and flexible fibrils with a diameter of 6-8 nm and a length of up to 200 nm observed by electron microscopy (77).

Synthetic Aβ with the arctic substitution (E22G) has been observed in the form of annular assemblies consisting of 40 to 60 molecules. The outer and inner diameter were 7-10 nm and 1.5-2.0 nm, respectively. The annular structure resembled pore-forming bacterial toxins and it was suggested that amyloid pores in the cell membranes might be the cause of the neuronal injury seen in Alzheimer's disease (78).

ADDLs are another result of preparation of synthetic peptide. They are small, globular structures, about 5-6 nm in size with a mass between 17-42 kDa. ADDLs consisting of Aβ(1-42) have proven to be neurotoxins, killing hippocampal neurons in a mouse brain slice model at nanomolar concentrations. They were also shown to bind cell surface proteins and to inhibit long-term potentiation (LTP)[1] (79).

Oligomers have further been extracted *in vivo* from cell cultures (75, 80) and from brains of mice (74) that express human forms of APP. The oligomeric forms were found to be SDS-resistant (75, 80) and have the ability to block LTP (80) and impair the memory (74) upon injection in rat brains. The causative agent of the memory loss was observed to be a 56-kDa soluble assembly of Aβ (Aβ*56), theoretically an Aβ(1-42) dodecamer (74).

[1] LTP is a measure on the strength of a chemical synapse, which is the basis for memory formation and learning (160).

1.7 Structure of Aβ(1-40) in different environments

Aβ(1-40) adopts varying conformations depending on the surrounding milieu. For example the method of preparation (like addition of the cosolvents dimethyl sulfoxide and trifluoroethanol), temperature, pH, time and presence of small molecules, for example detergent, are factors that affect the structure.

In dilute buffer of physiological pH at 25 °C, Aβ(1-40) is mainly monomeric and in random coil conformation (81). At decreasing temperature the conformation is somewhat changed and a weak form of secondary structure, termed polyproline II (PII) helix, is induced in the peptide, preferentially in the N-terminal part (residues 1-18) (82).

As mentioned, detergent induces structure in the peptide. It has also been shown that the detailed conditions for the detergent addition governs the adopted conformation for the peptide. Circular dichroism (CD) spectroscopy studies of Aβ(1-40) show that submicellar SDS concentrations accelerate the Aβ(1-40) aggregation and the peptide structure changes from random coil to β-sheet. At or close to the critical micelle concentration (cmc) (1-2 mM) the aggregation is at its maximum, visualized as β-structure by CD (83, 84). NMR studies on the same condition reveal line broadened signals indicating chemical exchange on an intermediate time scale and/or aggregation of peptide (84). The state also gives rise to ThT fluorescence which probably is due to the presence of amyloidogenic assemblies (83, 84)

By adding higher concentrations of SDS to reach the micellar state, the critical β-sheet state is passed and the induced Aβ aggregates are dissolved, at least partly. The Aβ(1-40) peptides associate to the micelles and concomitantly they adopt α-helical structure (83, 85, 86, 87). This α-helical state consists of two α-helices: an amphipathic helix made up of residues 15 to 24 and a hydrophobic helix constituted by residues 28 to 36 separated by a kink (residues 25 to 27). The two ends are flexible and consist of a long N-terminal part, amino acids 1 to 14, and a shorter, predominantly extended, C-terminal region, amino acids 37 to 40 (85, 86). Both helices are positioned inside the SDS micelle, the amphipathic helix closer to the headgroups of the micelle and the hydrophobic helix more deeply buried. The N- and C-terminal ends of the peptide are probably at the surface or outside the micelle (87).

It is difficult to use solution state NMR to visualize the β-sheet structure of Aβ since this state is so closely associated to formation of aggregates and large aggregates are not seen by NMR. The reason for this invisibility is line broadening of the signals probably due to fast transverse relaxation (88).

However, the Aβ(1-40) peptides can be trapped one by one in a β-hairpin conformation that is proposed to be the form that is adopted by Aβ in the fibrils (89). This entrapment is achieved by a so called Affibody molecule, a 58 amino-acid residue protein selected by phage display technology as an alternative to antibodies (90, 91). A dimeric construct of the Affibody molecule encloses Aβ(1-40), which folds into a β-hairpin with two hydrogen bonding β-strands (residues 17-23 and 30-36) and an unstructured N-terminal part (91).

1.8 Aβ and metals

Metals are often implicated in the discussion about the origin and development of Alzheimer's disease. The metal ions that are most often mentioned are copper, zinc and iron, which have essential functions in the body and the brain (92, 93).

Various cell types harbour and release zinc ions and one type is a glutamate-releasing neuron residing in cerebral cortex. The zinc ions are important in signalling and they are liberated in the synaptic cleft upon certain stimuli (94). Like zinc, copper is involved in neurotransmission. However, copper also has redox properties and can participate in the formation of reactive oxygen species (ROS), which in turn are able to harm various cell structures. This can develop into oxidative stress, a condition often seen in the Alzheimer's disease brain (93). The levels of zinc and copper are disturbed in the disease, with enhanced levels in the neuropil, especially in the plaques, compared to healthy people. Also the levels in serum and cerebrospinal fluid have been studied and deviations are observed (92, 93).

Copper and zinc ions have varying effect on Aβ peptide oligomer formation and aggregation *in vitro*, depending on several factors, for example pH (95) and concentration (96). Substoichiometric concentrations of Cu^{2+} have been seen to increase fibril formation and toxicity of Aβ(1-42), while higher concentrations increased formation of amorphous aggregates of less toxicity and increased precipitation (97). In another study high Cu^{2+} and Zn^{2+} concentrations increased precipitation of Aβ(1-40), while substoichiometric concentrations did not affect the precipitation significantly (96). The substoichiometric metal ion concentrations further transformed oligomeric assemblies into monomeric peptide (96).

Moreover, ThT and absorbance measurements have been used to study the aggregation of Aβ(1-40) and Aβ(1-42) in the presence of zinc and copper ions. Increasing concentrations of each metal ion resulted in decreased ThT fluorescence, indicating less β-sheet structure, while the absorbance also

decreased, indicating less soluble Aβ peptide. Hence, it was concluded that in the presence of the metal ions Aβ(1-40) and Aβ(1-42) form aggregates although they are of another character with a reduced β-sheet content (98).

The binding of zinc to Aβ has been studied by NMR around physiological pH (99). From ^{1}H 1D NMR spectra of Aβ(1-28) it was concluded that zinc ions bind to histidine 6, 13 and 14 and to the N-terminal amino group of the peptide (99). The same ligands were observed in an NMR study of the full length peptide Aβ(1-40) (100). A second binding site constituted by residues Asp23, Val24, Ser26 and Lys28 was also confirmed (100). Copper ions also show specificity for the histidine residues, but the binding to the N-terminal amino group and/or the side chain of Asp1 is a bit more uncertain (100, 101, 102).

1.9 Aβ and small molecules

There is yet no cure for Alzheimer's disease and available drugs only affect the symptoms. Even though the disease mechanism and the exact structure of the toxic unit still are hidden in the dark, much evidence suggests that formation of the soluble oligomers is at least one major cause for the disease. Accordingly, small molecules are highly interesting as modifying agents of the various oligomeric forms and aggregation processes or alternatively as stabilizers of monomeric Aβ (103). However, besides having affinity for Aβ in its monomeric or oligomeric form, the molecules have to fulfill requirements like being non-toxic and able to pass the blood-brain barrier (21). The interaction between Aβ and numerous small molecules are studied, both in applied research and in clinical tests, and hopefully this will reveal further information about the peptide aggregation and eventually end up in an effective treatment (21, 103).

Methods that are used to study the interaction between the peptide and small molecules are for example NMR, dot blotting, western blot, ELISA, ThT fluorescence, turbidity measurements, atomic force microscopy and transmission electron microscopy (104). In one study the small molecules tested were classified according to their influence on Aβ(1-42) oligomer and fibril formation, respectively, as seen by antibody techniques (104). Three groups were found: the first one included among others CR, ThT and curcumin and these compounds inhibited oligomers while fibrils still were formed. Compounds like lacmoid and phenol red belonged to the second group and they prevented both oligomer and fibril formation. The last category comprised for example direct red and orange g, which were fibril inhibitors although they did not affect the oligomer formation (104).

Another group of aromatic small molecules (including for example polyphenols) was found to structurally rearrange Aβ(1-42) soluble oligomers (105). The molecules could be grouped into three categories according to their effect on the oligomers. In one case the oligomers transformed into large assemblies, devoid of structure and toxicity. A different set of small molecules turned the soluble oligomers into ThT active fibrils with β-sheet structure and in the last category the soluble oligomers were induced to dissolve into smaller units with no structure or ThT activity (105).

2. Methods

2.1 Nuclear magnetic resonance spectroscopy

In 1945 the first discoveries were made leading to the development of nuclear magnetic resonance (NMR) spectroscopy, a very powerful and useful method (106, 107). In the field of protein science, NMR is used to investigate structure, dynamics, positioning and interactions. The method is based on the fact that the atomic nucleus has a quantum mechanical spin and in classical physics the property of spin involves a nuclear spin magnetic moment. Like a small bar magnet, the rotating charged nucleus gives rise to a small magnetic field oriented along the axis of rotation (108, 109).

The most spectacular thing in the modern NMR setup is the large superconducting magnet, giving rise to a static magnetic field, B_0. This strong field causes the magnetic moment to adopt different orientations, orientations that are connected to different energy levels. Each atomic nucleus with spin I has (2I+1) energy levels associated with it. These are degenerate in the absence of a magnetic field, but when the nuclei are subjected to a strong magnetic field, they are separated (108, 109).

For a spin half nucleus (I=1/2) there are two energy levels; the low-energy state (α state), when the magnetic moment is parallel to the applied magnetic field, and the high-energy state (β state), when the moment is antiparallel to the magnetic field. The population of the energy levels by the nuclear spins is determined by the Boltzmann distribution. It predicts that the α-state will be much more populated since it is associated with a lower energy. Hence, when all the spins in a sample are taken in account there will be a slight net alignment of the spins in one direction, i.e. parallel to B_0, at equilibrium. This net alignment of spins is described by the net magnetization vector **M** (108, 109). Introduction of this quantity brings the quantum mechanical description into a classical view.

By applying a small oscillating radiofrequency field, B_1, on the system, the net magnetization tilts away from B_0. In the classical description this causes the magnetization to precess, i.e. rotate, around B_0. The frequency of precession is

$$\nu_0 = -\frac{\gamma B_0}{2\pi} \quad (1)$$

and is called the Larmor frequency. γ is the gyromagnetic ratio and is specific for each type of nucleus. It is at the Larmor frequency that the nuclear spin transition takes place, which is visualized as an absorption peak in the spectrum after performed Fourier transformation (108, 109).

The NMR spectrum is expressed in the chemical shift scale, defined as

$$\delta(ppm) = 10^6 \frac{\nu_0 - \nu_{0,ref}}{\nu_{0,ref}} \quad (2)$$

where ν_0 is the Larmor frequency and $\nu_{0,ref}$ is the frequency of the line of a reference compound, for example tetramethylsilane (TMS). Each nucleus has a characteristic chemical shift due to a unique chemical environment. The B_0 field induces currents in the electrons surrounding the nuclei and these currents set up small magnetic fields opposing B_0. Every nucleus hence senses slightly different magnetic fields resulting in that different external magnetic frequencies are required to equal the Larmor frequency (108, 109).

A characteristic feature in the NMR spectrum is multiplet structure. This phenomenon is due to J-coupling between nuclei. The coupling is an interaction between two chemically bonded nuclei, mediated by the electrons in the bond. In this way magnetization can be transferred between nuclei (108, 109).

There are numerous different types of NMR experiments but they all have in common that the spins are manipulated, or disturbed, from the equilibrium position with radiofrequency pulses and field gradients.

2.1.1 2D experiments

Due to problems with resonance overlap, 1D NMR spectra often are very hard to interpret for complex molecules. Therefore 2D NMR methods are commonly used when studying small biological molecules. COSY (COrrelation SpectroscopY) and TOCSY (TOtal Correlation SpectroscopY) are homonuclear experiments giving information on nuclei that are connected through chemical bonds, while NOESY (Nuclear Overhauser Effect SpectroscopY) report on nuclei that are close in space (110, 111, 112). In constrast to the proton experiments just mentioned, the HSQC (Heteronuclear Single-Quantum Correlation spectroscopy) experiment is very useful when the peptide or protein is isotope labeled, often by ^{15}N or ^{13}C.

The two-dimensional HSQC experiment gives information about the chemical shift of a heteronucleus that is J-coupled to a proton and it is very useful when changes in the protein structure are of interest. In brief the HSQC experiment starts with an Insensitive Nuclei Enhanced by Polarization Transfer (INEPT) step that transfers magnetization from spin I, usually proton, to spin S, i.e. ^{13}C or ^{15}N (fig. 7). The S magnetization evolves during t_1, during which the nitrogen or carbon chemical shifts are probed, and is then transferred back to the I spin by a reversed INEPT step. The INEPT step and the final observation of proton results in a sensitivity gain (113). The resulting HSQC spectrum can be presented as a contour plot with the ^{13}C or ^{15}N frequency plotted versus the proton frequency.

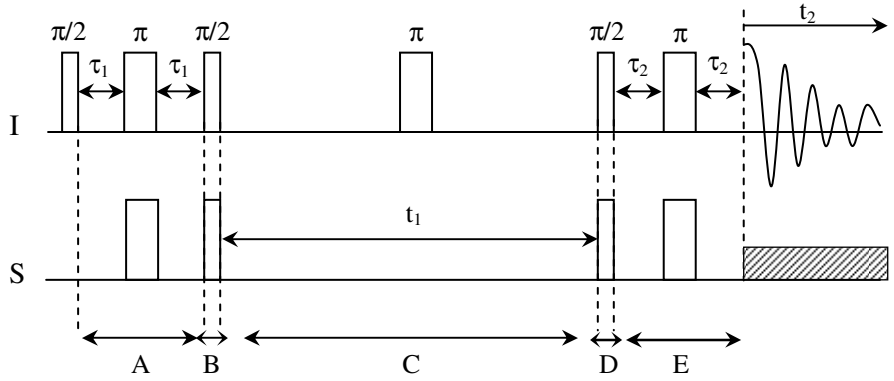

Figure 7. Pulse sequence of the HSQC experiment. Period A and B constitute an INEPT step during which proton magnetization is transferred to a low gyromagnetic ratio nucleus like ^{13}C or ^{15}N. During C the S spin magnetization evolves and is subsequently transferred back to the I spin during D and E that constitute a reversed INEPT step. In the acquisition period the S spin is decoupled (dashed rectangular box) to avoid heteronuclear splitting of the peaks (113).

A problem with solution NMR is that large proteins or complexes cannot be studied since the resonances become too broad due to slow tumbling, which results in a fast relaxation rate and a fast decay of the signal. However, the TROSY (Transverse Relaxation Optimized SpectroscopY) experiment is a way of dealing with larger proteins and reduces transverse relaxation rates. In the experiment only the narrowest component in a multiplet, the one that relaxes the slowest, is chosen and an improved spectrum is obtained (88, 108).

Another reason for loss of signal in NMR measurements is chemical exchange on an intermediate time scale. A peptide or a protein can adopt different conformations and when the molecule fluctuates between these states the corresponding resonances of the amino acids accordingly change posi-

tion. The rate of fluctuation is important for the outcome of the spectrum and if the rate is defined as slow, fast or intermediate depends on the size of the exchange rate in comparison to the chemical shift difference between the states. If the peptide slowly changes between two different conformations, there will be a double set of crosspeaks in the spectrum, representing each of the two different states. In contrast, if the exchange rate between the conformations is very fast then each amino acid will attain an average chemical shift of these two extremes. If the exchange rate between the states is intermediate however, the crosspeaks will be linebroadened to invisibility and little can be said about the condition (114).

2.1.2 Multidimensional experiments

Expansion of two dimensions to three and four has further developed the procedure of protein assignment and structure determination. These multidimensional NMR methods have made it possible to study proteins and assemblies of proteins of molecular mass around 25 kDa (115, 116).

2.1.3 Diffusion NMR

The translational diffusion experiment is highly useful when interactions between molecules are of interest. It also gives information about molecular size, shape, oligomerization state and protein folding (117). The experiment is based on the assumption that particles constantly are in random, translational motion and that this diffusion is very sensitive to changes in the hydrodynamic radius (r_H) of the molecule (81, 118). The relation between the diffusion coefficient and r_H is given by the Stokes-Einstein equation:

$$D = \frac{k_B T}{f} \tag{3}$$

$$f = 6\pi\eta r_H \tag{4}$$

where k_B is Boltzmann's constant, T is the absolute temperature, f is the coefficient of translational friction and η is the viscosity. The equation is valid for isotropic solutions assuming a spherical particle that strongly interacts with the surrounding liquid (118). Via the hydrodynamic radius the diffusion coefficient can be linked to the size of a peptide or a protein (81).

The technique of measuring diffusion is based on pulsed-field gradient (PFG) NMR introduced by Stejskal and Tanner, which in turn depends on the spin echo method by Hahn (119). The pulse sequence starts with a 90° pulse that flips down the equilibrium magnetization into the transverse plane and then a short and strong field gradient of strength g and duration δ is applied along the z-axis (fig. 8). The gradient causes the Larmor frequencies to

vary along the z-axis and phase differences between the spins, depending on their positions in the sample, are introduced (fig. 9) (117, 120). After the gradient there is a delay (Δ) followed by a 180° refocusing pulse, which inverts the phase shifts. Finally there is another gradient, identical to the first one (117, 120).

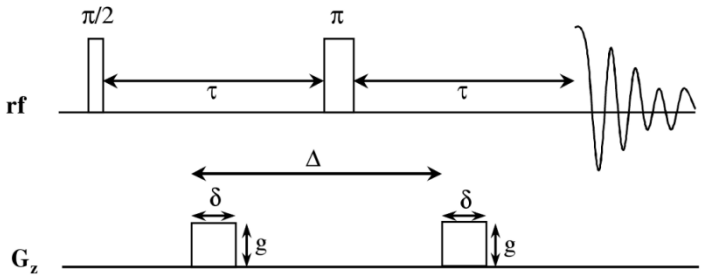

Figure 8. Pulse sequence for translational diffusion NMR. The transverse magnetization, generated by a 90° pulse, is first subjected to a gradient of strength g and duration δ. During the delay Δ a 180° pulse is applied and before acquisition there is another gradient, identical to the first one (117).

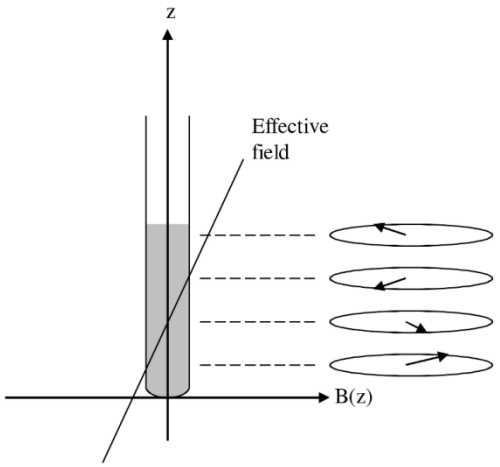

Figure 9. Schematic picture illustrating an NMR sample that is exposed to a field gradient that causes the magnetic field to vary over the sample. The varying magnetic field results in slightly different Larmor frequencies along the sample.

If the spins do not move during the delay, the phase shifts introduced during the first gradient will be refocused by the second gradient pulse. However, this is not the case if the spins diffuse during the delay (119). Then they are dephased and the result is a decreased signal when all the phase-shifted magnetization vectors are added up. Spins that diffuse faster move longer distances and they will be affected by larger changes in the magnetic field. This causes a larger variation in the phases and a greater loss in signal (120).

The relation between the measured intensity of the NMR signal and the diffusion of a spin is given by the Stejskal-Tanner equation (119):

$$\frac{S(2\tau)}{S(0)} = e^{-\gamma^2 D\delta^2(\Delta-\frac{1}{3}\delta)g^2} \qquad (5)$$

where $S(2\tau)$ represents the measured signal intensity after a diffusion time Δ and a gradient strength g, while S(0) is the intensity without gradients. γ is the gyromagnetic ratio, D is the diffusion constant and δ is the length of the gradient pulse (119). The diffusion constant is determined by repeating the diffusion experiment with varying g, Δ or δ.

2.2 Circular dichroism spectroscopy

Circular dichroism (CD) spectroscopy is a method that gives information about secondary structure of proteins and peptides. The method relies on the fact that chiral molecules absorb left and right circularly polarized light to different extents, a phenomenon called circular dichroism (121).

The sample is illuminated with plane polarized light that can be considered as a sum of equal parts of left and right circularly polarized light. If one of the circularly polarized components is absorbed more than the other upon passing through the sample, the outcoming resulting light will be elliptically polarized (fig. 10). The two components of the incident light can also be slowed down differently due to differences in refractive index, resulting in that the plane of the plane polarized light is rotated by an angle α (fig. 10). This phenomenon is described as optical rotation (121, 122, 123).

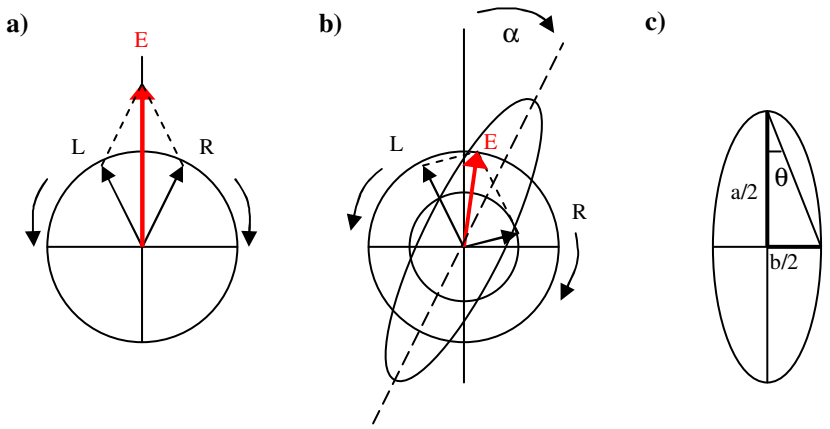

Figure 10. a) The light reaching the sample is plane polarized and the electric field vector (E) consists of two counter-rotating components (L and R, left and right circularly polarized light). b) The light has passed through a sample of molecules that absorb left and right circularly polarized light differently. When adding the components the resulting light is elliptically polarized. The ellipse has been rotated by an angle α due to optical rotation. c) Ellipticity, θ, is defined as arctan(b/a) and is a quantity to describe the degree of circular dichroism (121, 122, 123).

The measured signal in CD is

$$\Delta A = A_L - A_R = \varepsilon_L lc - \varepsilon_R lc = \Delta\varepsilon lc \qquad (6)$$

where A_L and A_R are the absorptions of left and right circularly polarized light, respectively, ε is the extinction coefficient, l is the sample path length and c is the sample concentration. Ellipticity, θ, is another quantity used and the angle is shown in figure 10. It is calculated as $\theta = \arctan(b/a)$ (122, 123).

Generally, CD for a protein or a peptide is reported in the unit mean residual molar ellipticity, [θ]:

$$[\theta] = \frac{\theta_{obs}}{10 \cdot c \cdot l \cdot n} \qquad (7)$$

θ_{obs} is the observed ellipticity (mdeg), c is concentration (mol/l), l is the path length of the cuvette (cm) and n is the number of residues in the peptide or protein. The unit is deg·cm^2· dmol^{-1} (121, 122, 123).

In far-UV CD, i.e. CD measurements performed below 250 nm, the main chromophore in peptides and proteins is the amide group in the peptide bond

(124). The electronic transitions are nπ* at about 220 nm and ππ* at about 190 nm. Since the amide group constitutes the backbone in peptides and proteins, the CD signal gives very good information about the secondary structure (123). α-helical secondary structure is represented by a curve with a maximum at 193 nm and two minima at 208 and 222 nm, respectively. β-sheet structure is recognized as a curve with a maximum at 195 nm and a minimum at 215 nm. Random coil is characterized by a minimum at 197 nm (125). The different secondary structures are exemplified in figure 11 (126).

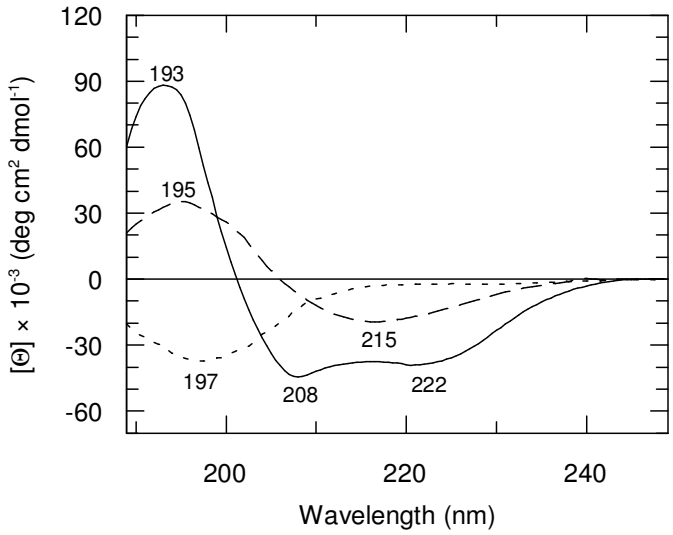

Figure 11. Shapes of CD spectra measured for various secondary structures; α-helix (black line), β-sheet (long dashes) and random coil (short dashes) (126).

2.3 Fluorescence spectroscopy

Fluorescence is a form of luminescence, i.e. emission of light from an excited state of a molecule, the fluorophore. Possible events occurring after a fluorophore has been excited through absorption of energy are described by the Jablonski diagram (fig. 12). Upon excitation from the electronic ground state, also called a singlet state, S_0, a vibrational energy level (0, 1, 2, etc) in the first (S_1) or second (S_2) electronic state is reached. Then the fluorophore relaxes to the lowest vibrational level within S_1, a process happening in the picoseconds timescale and called internal conversion. Afterwards, and usually more slowly, the molecule relaxes to the electronic ground state by emitting a photon, the actual process that is registered by the spectrometer as fluorescence (127, 128).

Relaxation can also occur by for example quenching and energy transfer, events that do not result in photon emission. The fraction of molecules that deexcites through fluorescence is called the fluorescence quantum yield (Φ_F). Phosphorescence is another form of luminescence but it involves forbidden transitions between the energy levels (from a singlet state to a triplet state) and is therefore a much slower process than fluorescence. The resulting emission rate is typically 10^3-10^0 s^{-1} in phosphorescence and 10^8 s^{-1} in fluorescence (127, 128).

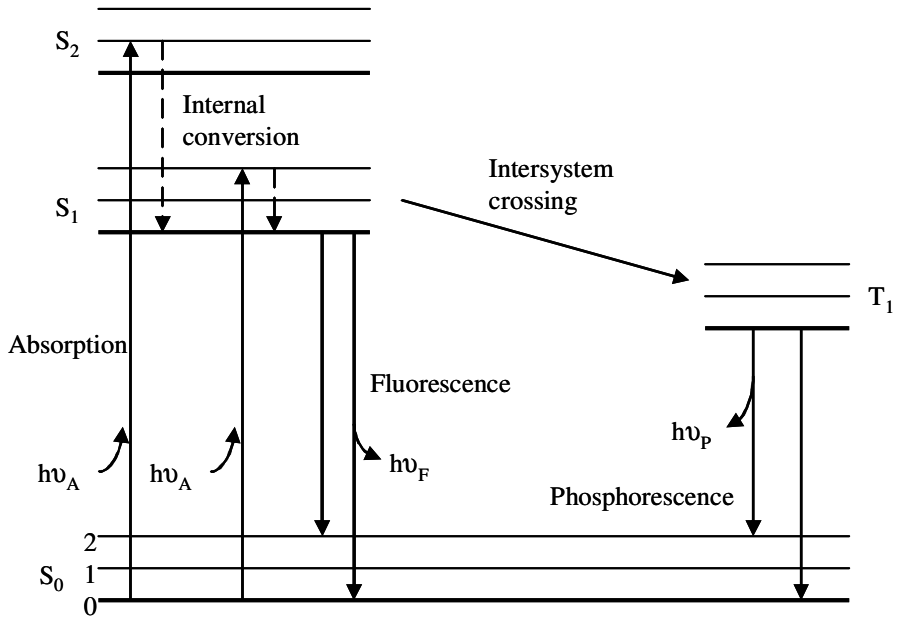

Figure 12. A Jablonski diagram showing the possible events that occur after a fluorophore has been excited through absorption of energy ($h\upsilon_A$, where h is Planck's constant and υ_A is the frequency of absorption) (after (127)). S_0 is the electronic ground state while S_1 and S_2 are the first and second electronic states. 0, 1 and 2 indicate the vibrational energy levels within the electronic states. Phosphorescence is a slower process than fluorescence since it involves emission of light from a triplet excited state (T_1) to the ground electronic state, a forbidden process (127).

When proteins and peptides are studied by fluorescence spectroscopy the presence of aromatic residues or external probes are necessary. Tryptophan, tyrosine and phenylalanine side chains all show fluorescence and tryptophan has the strongest emission. They have somewhat different absorption and emission spectra, with phenylalanine absorbing at the shortest wavelength and tryptophan at the longest. Usually the measurements are performed at an

excitation wavelength of 280 nm, resulting in that only tryptophan and tyrosine are excited (127). Examples of extrinsic fluorophores that can be attached to the molecule of interest are fluorescein and green fluorescent protein (GFP) (127, 128).

2.4 Membrane mimicking environments

Many proteins and peptides that are studied for information about their structure are in their native environment either integrated in the cell membrane or associated to the membrane surface (129). The cell membrane is a very complex system arranged as a bilayer constituted by different lipids supporting the proteins. To obtain information about the native structure of a protein or a peptide it is important to mimic the cell membrane to the greatest extent possible. However, the method of high resolution NMR in solution limits the different systems that can be used in order to determine the structure of an associated peptide (129). A big complex in the context of NMR measurements is »10^5 Da and consists of for example a protein or a peptide bound to a phospholipid bilayer in the form of a vesicle or a multilayer. This assembly moves so slowly that the resonances will be broadened to invisibility in the NMR spectrum (130). Detergent micelles on the other hand are often smaller (about 10^4 Da) and offer a good substitute for the membrane interface (129, 130). An even better membrane mimicking environment is offered by so called bicelles or mixed micelles, although they are generally somewhat larger than micelles (131, 132).

2.4.1 Micelles

Detergents are amphiphilic molecules with a hydrophilic head group (ionic, non-ionic or zwitterionic) and a hydrophobic tail. In aqueous solution the detergents self-associate and form micelles, i.e. assemblies resembling spheres where the headgroups form the outer surface enclosing the hydrophobic tails directed inwards. The micelles are distributed in the solvent and are in rapid equilibrium with the soluble detergent monomers. The critical micelle concentration (cmc) is the minimum concentration needed for micelles to form. The cmc depends among other things on the chemical structure of the monomer, temperature, pH and ionic strength (129, 133).

When peptides are going to be studied in a membrane mimicking environment by solution NMR, SDS micelles are an alternative. SDS is a detergent with a linear alkyl chain and a negatively charged headgroup (fig. 13). It forms micelles consisting of in average 62 molecules with an unhydrated radius of about 28 Å at 25 °C (87, 129).

An advantage with SDS micelles is that they are small enough to move fast and isotropically, giving high-resolution NMR spectra (50). Although SDS micelles are a common system for folding of surface-active peptides, its use has been questioned, mainly because it promotes protein-protein hydrogen bonds and solvates hydrophobic side chains, resulting in β-sheet structures (134).

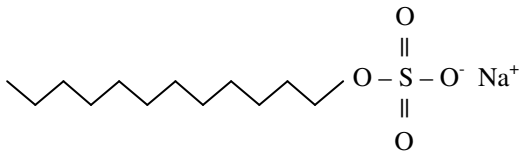

Figure 13. The chemical structure of an SDS molecule (129).

The solubility of SDS is very much influenced by the temperature and at about 16 °C, depending on concentration and the presence of ions, it precipitates rapidly. When performing studies at low temperatures lithium dodecyl sulfate (LiDS) is better to use due to higher solubility (129, 135). The cmc of LiDS is slightly higher than the one for SDS, (8.8 mM in comparison to 8.1 mM), but the two salts have been found to be equivalent (129, 136). Examples of other molecules forming micelles are the positively charged dodecyltrimethylammonium chloride (DTAC) and the zwitterionic, neutral, dodecylphosphocholine (DPC) (50).

3. Results and Discussion

The five papers included in this thesis concern interactions between Aβ(1-40) and selected molecules with varying properties and metal ions. In all projects the β-sheet structure has been of central importance, the structure that is believed to be strongly connected to the neurotoxic species in Alzheimer's disease.

The β-sheet structure is difficult to catch by NMR, probably since it is so closely linked to formation of larger aggregates and chemical intermediate exchange between different states of the Aβ peptide. Therefore other methods like CD, fourier transform infrared (FTIR) spectroscopy and ThT fluorescence have given valuable complementary information.

In paper I-III the β-sheet structure is induced and stabilized by detergent, CR and an Affibody molecule, respectively. The β-sheet state is not observed by NMR in paper I and II in contrast to the study in paper III.

Both the detergent molecules SDS and LiDS and the dye CR are negatively charged but still they interact with Aβ(1-40), which is also negatively charged at physiological pH. Probably hydrophobicity is a strong driving force for interaction, especially in the case of the detergent molecules.

In paper I the β-sheet state is induced at the condition of 75 μM peptide and 1-2 mM detergent, i.e. at a ratio of 1 peptide to 13-26 detergent molecules. Tentatively interaction occurs between various forms of both the peptide and the detergent; monomeric molecules as well as molecules organized in assemblies.

For the Aβ-CR interaction we speculate that the positively charged lysines at position 16 and 28 in Aβ(1-40) are of major importance. The dimensions of the CR molecule, with its negative charges at the ends, match these amino acid residues when Aβ(1-40) is in a β-hairpin conformation, resulting in ionic interactions.

In paper III Aβ(1-40) is locked one by one in a β-hairpin conformation by the interaction with two Affibody molecules (cf 89). This state is actually visible by solution NMR. The structure is very similar to the one determined

for Aβ situated in fibrils found earlier by solid state NMR (137). Here the interaction is different from the one in paper I and II; while the detergent molecules and CR probably are in monomeric as well as in smaller and larger assemblies upon interaction with Aβ, the Affibody molecule surrounds the peptide.

In paper IV the central part is once again β-sheet structure. But here the view is somewhat different and the work leads to the question of what amyloid really means and what it is characterized by. The interaction between Aβ(1-40) and an engineered β-cyclodextrin dimer is studied by NMR and by a kinetic aggregation assay using ThT. NMR measurements confirm the interaction and reveal a millimolar dissociation constant. The kinetic assay records continuously the Aβ aggregation and the cyclodextrin dimer is observed to modulate the process in a concentration dependent manner.

In paper V the influence of the metal ions Cu^{2+} and Zn^{2+} on Aβ(1-40) at various pHs is studied. It is observed that while Cu^{2+} ions still show ligand specific binding involving the histidine residues in the N-terminal part of the peptide at decreasing pH, the Zn^{2+} ions gradually lose or change their residue specific binding.

Overall my research shows that the Aβ peptide conformation is very sensitive to the environment and that it easily adopts varying states depending on the surrounding conditions. This may be one reason for its connection to Alzheimer's disease; that it is prone to adopt varying conformations and that its environment leads it into a misfolded state.

3.1 Paper I

Secondary structure conversions of Alzheimer's Aβ(1-40) peptide induced by membrane-mimicking detergents

The purpose of this work was to study and characterize the oligomeric state of the Aβ(1-40) peptide. This state is suspected to comprise the neurotoxic species in Alzheimer's disease, and many projects have been dedicated to this condition. The detergent induced structural conversions of Aβ have been studied earlier (84, 138), but not at the detailed level as in this work.

Since Aβ originates from a transmembrane protein and even partly comes from the membrane spanning part, it is in close proximity to the cell membrane. Membranes also have been suggested to be important in the aggregation process of the peptide (139). To take this into account the study involved the detergents SDS or LiDS as a membrane mimetic system, also proposed to be a model system for peptide aggregation (134).

The detergent was added to the peptide solution in small amounts and the structural changes of the peptide were followed by different NMR experiments, CD, FTIR, ThT fluorescence and native-PAGE. The NMR ^{1}H-^{15}N HSQC experiments were run at 3 °C since the amide crosspeaks were better defined at low temperature due to slower exchange of the amide protons with the protons in the water molecules.

The experiments suggest that the oligomeric state of the peptide, induced by 1-2 mM detergent concentration, were stabilized. At this concentration of detergent the CD spectra at 3 and 20 °C showed a secondary structure dominated by β-sheet. The same conditions studied by NMR revealed a ^{1}H-^{15}N HSQC spectrum with complete signal loss. When analyzing the volume of each amino acid with increasing LiDS concentration, we could see that the signal from each amino acid was mainly unchanged at concentrations up to 500 μM, but then it abruptly decreased at 1 mM and finally completely disappeared at 2 mM. With increasing detergent concentration the signals reappeared, the amino acids in the C-terminus with strongest intensity, but at entirely different chemical shifts. The new chemical shifts indicated α-helical regions in the peptide (87).

Loss of signals in NMR can be due to a variety of reasons. The apparent explanation here is that large assemblies of peptide and detergent are formed. Big aggregates have a very slow tumbling rate that results in a fast relaxation rate, in turn giving very broad and therefore invisible peaks (88). However, another possibly additional explanation could be chemical exchange on an intermediate time scale between aggregates of different sizes

and conformations including monomers. This was proposed in a paper by Schulman *et al* where they studied the unfolding of α-lactalbumin in the form of a molten globule (140). The molten globule is a state during the folding of a protein where the secondary structure elements have formed, but the tertiary state has not yet settled and the structure is somewhat loose. α-lactalbumin was monomeric but only 3 out of 122 residues were seen in the NMR spectrum, a fact that was attributed to conformational fluctuations on a millisecond time scale. All residues were not observed until highly denaturing conditions were applied (140).

In an attempt to shed more light on the question of resonance disappearance, our Aβ samples were analyzed by native-PAGE. The preliminary results show that in the presence of 1 and 2 mM SDS, there are high molecular mass complexes in the samples. This strengthens the observations that oligomeric states are induced at 1-2 mM detergent concentration, although chemical exchange cannot be excluded as an additional factor.

Further NMR experiments were run to study this "invisible" state. A TROSY HSQC experiment, designed to give higher NMR intensity to high molecular mass systems, revealed weak resonances with chemical shifts agreeing well with the chemical shifts of the amide crosspeaks of valine 39 and valine 40. This indicates a higher mobility in the C-terminus of the peptide, which is a bit surprising since the end is hydrophobic and is expected to be buried in the interior of the complex. However, an alternative explanation to the appearance of valine 39 and 40 in the TROSY spectrum could be that the crosspeaks of these C-terminal amino acids in general have a strong intensity, also in this experiment.

Diffusion NMR could not give any valuable information about the state in the presence of 2 mM SDS since the signals were lost. However, when the peaks started to gain intensity again, the monomeric initial state had been transformed into a state with a slower diffusion coefficient, indicating that assemblies of peptide and detergent molecules had formed.

The "invisible" Aβ intermediate state was further investigated by performing the detergent titration in the presence of ThT and the induced fluorescence was measured. The method of measuring ThT fluorescence as an indication of presence of amyloid material is widely used, even if it is not known to what structure the dye actually binds (58, 141). We could show that the state characterized as β-sheet structure by CD and signal loss by NMR was ThT active and gave rise to maximal fluorescence during the titration.

The peptide in only buffer, or in the presence of low detergent concentrations, was mainly unstructured, with a contribution of PII helix at low temperature. This is in accordance with earlier work (82). The state adopted in

high detergent concentration is also well characterized: two α-helices, comprising amino acids 15-24 and 29-35 respectively, are induced in the peptide structure. The first helix is positioned closely to the headgroups in the micelle while the C-teminal helix is located further inside (87).

The results from the FTIR measurements were generally consistent with the findings from the other methods. However, the indicated presence of β-sheet also in the initial measurements when Aβ(1-40) was dissolved in only buffer and when 0.1 mM SDS had been added was somewhat surprising. The question is if this β-sheet initially exists in all measurements, although it cannot be visualized by CD or NMR.

In summary, a broad range of methods were used to characterize the oligomeric state of Aβ(1-40) induced by SDS or LiDS. There is much to suggest that high molecular mass complexes are formed at detergent concentrations of 1-2 mM. They are β-sheet rich, ThT active and "invisible" in ^{1}H-^{15}N HSQC experiments. The TROSY experiment indicates a higher mobility in the C-terminus of the peptide. How the assembly of peptide and detergent is organized and what size the complex actually has, are very interesting questions.

In one attempt to learn more about the oligomeric Aβ structure induced at 2 mM detergent, the short peptide KKLVFFA was titrated into the sample in a preliminary experiment. KLVFF is found in the Aβ amino acid sequence (residues 16-20) and has been seen to bind to Aβ(1-40) and interfere with Aβ fibrillation (142). Upon KKLVFFA addition, in a molar ratio of 1:1 with respect to Aβ(1-40), some crosspeaks of the peptide reappeared in the ^{1}H-^{15}N HSQC spectrum. Further addition of KKLVFFA caused all Aβ(1-40) crosspeaks to come back at the initial random coil chemical shifts, although with a reduced intensity.

One can only speculate about what happens when KKLVFFA is added to the sample containing peptide and detergent in a ratio resulting in the "invisible" state. If it is assumed that Aβ molecules are surrounded by detergent molecules, will then the positively charged KKLVFFA bind to the negatively charged detergent molecules and pull them out of the complex? This could result in a decreased available concentration of detergent and make it possible for Aβ(1-40) to adopt its initial random coil state once again. If it is the other way around, that Aβ is surrounding detergent molecules, then KKLVFFA may interact with the peptide itself, disturbing its association to the detergent assembly. The complex of peptide and detergent could also be a randomized association, disturbed or dissolved by KKLVFFA.

3.2 Paper II

Detergent-like interaction of Congo red with the amyloid β peptide

Paper II has the same focus as paper I, but instead of detergent, CR was titrated onto Aβ(1-40) and induced structural changes were followed by NMR, CD, absorbance measurements, dynamic light scattering (DLS) and electron microscopy.

When incubated with soluble Aβ(1-40), CR has been shown to inhibit fibril formation and concomitantly abolish the neurotoxic effect of the peptide in a primary rat hippocampal culture. Furthermore, CR prevented the neurotoxic effect of already formed fibrils (66). In a *Drosophila* model expressing Aβ(1-42) the number of plaques was decreased and the life time of the flies was prolonged when the dye was mixed with their food (143). However, CR has been seen to have a variable influence on protein aggregation depending on its concentration. In a study of an amyloid forming protein (the amyloidogenic immunoglobulin light chain variable domain) CR in low concentrations promoted formation of β-sheet containing fibrils and aggregates. In contrast, CR present in high concentration reduced the aggregation of the protein. The proposed reason for the observed effects is that CR in low concentrations induce partially unfolded, aggregation prone forms of the protein while in high concentrations it causes protein unfolding, a state less ready for aggregation (144). In accord with this it has been proposed that CR binds to Aβ(1-40) by a two-state mechanism and that CR in a 1:1 ratio increases peptide aggregation while a high CR concentration has an aggregation reducing effect (145).

The aggregation modulating properties of CR (144, 145), in combination with its proposed micelle-like behaviour that resembles the ones of detergents (57), inspired us to the present study.

CR was titrated onto Aβ(1-40) peptide, starting at substoichiometric concentrations and ending at a 10-fold molar excess. The CD measurement gave information about a structural conversion from the initial random coil state to a state composed of both random coil and β-sheet. In similar ways both CR and SDS/LiDS hence induced β-sheet containing structures in Aβ although CR could not induce the formation of the final α-helical state of the peptide.

In the same way as the CD measurement, the ^{1}H-^{15}N HSQC experiments revealed an initial very similar behaviour of Aβ(1-40) in the presence of

increasing concentration of detergent and CR. Common to both agents is that they induced disappearance of the Aβ(1-40) crosspeaks. Further, in both cases the most C-terminal residues were the least affected. The phenomenon of peak loss can have several explanations. As described in "Results and Discussion" of paper I, large aggregates are invisible in NMR spectra since the signal fades too quickly due to fast transverse relaxation rates (88). Another reason is chemical exchange on an intermediate time scale (114).

By adding detergent the invisible state can be passed and the chemical shifts of the crosspeaks report on an α-helical state, but this did not happen in the presence of increasing concentration of CR. The crosspeaks were still lost. These results indicate an essential mechanistic difference between detergent and CR and that CR lacks the strong solubilising property of SDS and LiDS.

Possibly CR induces a state of the peptide, or locks the peptide in a state, that consists of lots of peptides and dye molecules forming a huge complex. Alternatively various small assemblies are formed in which Aβ fluctuates on an intermediate timescale between different conformations.

CD studies, absorption spectroscopy, DLS and transmission electron microscopy gave indications that CR accelerates formation of β-sheet-containing aggregates in comparison to Aβ(1-40) alone in buffer.

A possible model of how CR and Aβ(1-40) interact may be that the peptide adopts a β-hairpin conformation and that the dye is positioned along the formed structure. This would allow ionic interaction between the negatively charged sulfonate groups in CR and the positively charged lysines (residues 16 and 28) in Aβ. The β-hairpins could then gradually assemble in larger aggregates.

It is interesting that our results, as well as the results of others (146), show an increased aggregation of Aβ in the presence of CR simultaneously as there are observations about a decreased Aβ neurotoxicity when CR is added (66, 143). Hypothetically the increased aggregation could be due to that CR binds to the initially monomeric peptide and induces the β-hairpin structure. The peptide in β-hairpin structure could then assemble in the protofilament structure proposed by Lührs *et al* (137). In this model the Aβ peptide has the shape of a β-hairpin and then several hairpins are stacked on top of each other forming two intermolecular parallel, in-register β-sheets (137). However, the reduced toxicity of the peptide in presence of CR probably reflects a modified structure of the peptide assembly. This could be due to the detergent-like property of CR, which might modulate the size of the formed fibrillar aggregates or the surface of the aggregates. Another possibility is that

CR directs the peptide aggregation into a different pathway, avoiding formation of toxic oligomers (146).

3.3 Paper III

N-terminal engineering of amyloid-β-binding Affibody molecules yields improved chemical synthesis and higher binding affinity

Paper III deals with Aβ(1-40) and the Affibody molecule, a protein that was developed as an alternative to antibodies. It consists of 58 amino acids in the original form, is organized in three helices, and originates from the Z domain of the immunoglobulin binding staphylococcal protein A (SPA). The Affibody molecule gets its high affinity for a specific molecule by randomizing 13 amino acids in its sequence by phage display from combinatorial libraries (147). An Affibody molecule, $Z_{Aβ3}$, with nanomolar affinity for the Aβ peptide has been selected as a possible therapeutics for Alzheimer's disease or as an analytical tool (89, 91).

$Z_{Aβ3}$ binds as a dimer to monomeric Aβ(1-40) and upon binding both molecules fold (89). Aβ(1-40) is enclosed by the Affibody dimer and adopts a β-hairpin conformation comprising residues 17-36, residues 17-23 and 30-36 form β-strands. Both $Z_{Aβ3}$ and Aβ(1-40) have unstructured N-terminal ends (89). Interestingly, the capture of Aβ by the Affibody dimer makes it possible to visualize the peptide in the β-sheet structure state by NMR (89). This is fascinating since the aggregated β-sheet states induced by detergent and CR in paper I and II are invisible by NMR. A consequence of the Affibody binding to Aβ is that the peptide is kept in a monomeric form and is prevented from aggregation (89). The structural model of Aβ(1-40) in complex with the Affibody dimer (89) is strikingly similar to the model of Aβ(1-42) in fibrils based on a combination of solution and solid state NMR (137). In this model Aβ(1-42) adopts a β-strand-turn-β-strand conformation in which residues 18-26 and 31-42 form the β-strands and the N-terminal 17 residues are non-structured (137).

The purpose with paper III was to generate $Z_{Aβ3}$ synthetically, instead by expressing it in *Escherichia coli*, and optimize its yield by N-terminal truncation. However, although truncated, the $Z_{Aβ3}$ molecule should retain its affinity for Aβ(1-40). The characterization of the synthesized Affibody molecules bound to Aβ(1-40) was performed by CD, surface plasmon resonance (SPR)-based biosensor analysis and NMR.

Seven variants of the Affibody molecule were synthesized; $Z_{A\beta3}$(1-58), $Z_{A\beta3}$(3-58), $Z_{A\beta3}$(6-58), $Z_{A\beta3}$(9-58), $Z_{A\beta3}$(12-58), $Z_{A\beta3}$(15-58) and $Z_{A\beta3}$(18-58). The more truncated, the higher the yield of the molecule. CD, SPR and NMR all showed in accord that $Z_{A\beta3}$(12-58) and $Z_{A\beta3}$(15-58) kept the affinity for Aβ(1-40) while $Z_{A\beta3}$(18-58) lost it. The three amino acids $E_{15}I_{16}V_{17}$ are hence very important for the affinity of $Z_{A\beta3}$ for Aβ. This is in agreement with earlier results showing that residues 15-18 form a β-strand that hydrogen bond to Aβ(1-40) and obviously this part is very important for the interaction to occur.

The CD spectrum of $Z_{A\beta3}$(1-58) showed α-helical structure, which is in accordance with earlier reported data that two of the three helices are retained when the Affibody molecule is in its free form, while the N-terminal helix gets disordered (148). When Aβ(1-40) was titrated onto $Z_{A\beta3}$(1-58) the α-helical signal was decreased and the same was observed for the samples of $Z_{A\beta3}$(12-58) and $Z_{A\beta3}$(15-58) in the presence of increasing concentration of Aβ(1-40). In addition, contribution of β-sheet structure could be discerned in the two latter cases. The CD spectrum of $Z_{A\beta3}$(18-58) and increasing concentration of Aβ(1-40) did not show any significant changes.

Interestingly, both melting curves and SPR measurements indicated that $Z_{A\beta3}$(12-58) and $Z_{A\beta3}$(15-58) have a stronger affinity for Aβ(1-40) than the full length Affibody molecule; the dissociation constants are 0.69 nM and 0.48 nM for $Z_{A\beta3}$(12-58) and $Z_{A\beta3}$(15-58) binding to Aβ(1-40), in comparison to 9.5 nM for $Z_{A\beta3}$(1-58).

The ^{1}H-^{15}N HSQC spectra of ^{15}N-labeled Aβ(1-40) in the presence of molar excess of unlabeled Affibody molecules strengthened the already discussed results; $Z_{A\beta3}$(1-58), $Z_{A\beta3}$(12-58) and $Z_{A\beta3}$(15-58) form complex with Aβ(1-40) while $Z_{A\beta3}$(18-58) does not show any affinity for the peptide. The complex formation between the various Affibody molecules and Aβ(1-40) was seen as dispersed crosspeaks in the HSQC spectra, indicating induced β-strands in residues 18-24 and 30-36 of the Aβ peptide. This is in general agreement with earlier results of Aβ(1-40) and $Z_{A\beta3}$(1-58) (89). When carefully comparing the chemical shift changes in Aβ(1-40) induced by $Z_{A\beta3}$(1-58), $Z_{A\beta3}$(12-58) and $Z_{A\beta3}$(15-58), respectively, $Z_{A\beta3}$(12-58) and $Z_{A\beta3}$(15-58) induced very similar changes in the peptide as the full length Affibody molecule. However, $Z_{A\beta3}$(12-58) gave Aβ chemical shift changes somewhat more similar to $Z_{A\beta3}$(1-58) than $Z_{A\beta3}$(15-58) did.

The study shows that by N-terminally truncating the Affibody molecule the yield in the chemical synthesis is greatly improved, to about 30% for $Z_{A\beta3}$(12-58) and $Z_{A\beta3}$(15-58), in comparison to 8% for $Z_{A\beta3}$(1-58). Further-

more, the affinity for the Aβ(1-40) peptide gets higher by truncation, possibly by less steric hindrance when the disordered N-terminal part is removed. The ^{1}H-^{15}N HSQC spectra show that although 11 to 14 amino acids of the Affibody molecule are removed, the truncated variants induce about the same structure in Aβ(1-40) as $Z_{Aβ3}$(1-58) does.

3.4 Paper IV

Specific binding of an engineered β-cyclodextrin dimer to the amyloid β peptide modulates the peptide aggregation process

Paper IV is a continuation of a study on Aβ and cyclodextrin monomers (149). Cyclodextrins are cyclic, cone shaped molecules that consist of varying number of glucopyranose units. The most common forms are α-, β- and γ-cyclodextrin with six, seven and eight glucopyranose units, respectively. The different sizes result in varying characteristics concerning solubility, stability and flexibility (150).

An advantage with cyclodextrins is that due to their hydrophilic exterior and hydrophobic interior they are suitable for host-guest interactions (150). Typically the cyclodextrin surrounds a benzene group of the guest molecule. This host property in combination with non-toxicity of several derivatives has made cyclodextrins common ingredients in drugs, food and cosmetics to increase stability and/or solubility (151).

There are earlier studies on Aβ and cyclodextrin that report that β-cyclodextrin interacts with Aβ(12-28) (152) and Aβ(1-40) (149, 153), which results in reduced fibrillation (152, 153) and neurotoxicity (153, 154).

The interacting sites between β-cyclodextrin and Aβ have been shown by NMR studies to be V18 (152), Y10 (149) and F19 and/or F20 (149, 152). Especially the phenylalanines have proven to be important for binding to occur (149). The dissociation constant for the binding between Aβ(1-40) and β-cyclodextrin is 3.9±2.0 mM as measured by translational diffusion NMR spectroscopy (149).

Besides these reports on interaction between β-cyclodextrin and Aβ and the resulting reduced Aβ aggregation, there are studies showing opposite effects. In one study ThT fluorescence and turbidity measurements indicated that β-cyclodextrin does not inhibit Aβ aggregation but merely prevents binding of ThT to the fibrils (104). Another study with ThT measurements found that

β-cyclodextrin in low concentration promotes Aβ fibril formation, while in high concentration it has an inhibiting effect (155).

We have investigated the interaction between an engineered β-cyclodextrin dimer and Aβ(1-40) by NMR and we have also measured the effects of the β-cyclodextrin monomer and the dimer on the kinetics of Aβ aggregation.

The idea behind the synthesis of a β-cyclodextrin dimer was that dimerization would increase the cyclodextrin affinity to the peptide since there are more than one binding site in Aβ(1-40) for the β-cyclodextrin monomer. Hypothetically, after one monomer in the cyclodextrin dimer has bound to Aβ(1-40), the other monomer would probe the possible binding sites in the peptide and then more easily attach.

By translational diffusion measurements the cyclodextrin dimer was found to have a somewhat stronger affinity for Aβ(1-40) than the monomer. The dissociation constant was decreased from 3.9±2.0 mM (149) to 1.1±0.5 mM.

^{1}H-^{15}N HSQC measurements showed that the crosspeaks for Y10, F19 and F20 shift when the β-cyclodextrin dimer is titrated onto Aβ(1-40). However, D7 and L17 showed comparable induced chemical shift changes. In fact the N-terminal amino acid residues in general were affected by the presence of the β-cyclodextrin dimer. Interestingly, the histidines in Aβ(1-40) also showed induced chemical shift changes as visualized by ^{1}H-^{13}C HSQC spectra. This information could not be obtained from the ^{1}H-^{15}N HSQC spectra since the amide crosspeaks of the histidines are not visible at pH 7.4. Further, a ^{1}H-^{13}C HSQC spectrum of Aβ(1-40) with the β-cyclodextrin monomer also showed induced chemical shift changes of the histidines.

That all aromatic amino acid residues in the peptide showed induced chemical shift changes in the presence of cyclodextrin, irrespective of monomeric or dimeric form, brings up the suggestion that the aromatic ring structures are surrounded by the cyclodextrin cavity (152).

The kinetic aggregation experiments gave another perspective of the interaction between Aβ and the β-cyclodextrin monomer and dimer, respectively. While the NMR measurements were performed during a short time period the aggregation experiments followed the complete aggregation process of the peptide. Probably the NMR measurements reflect the behaviour of the peptide during the corresponding lag phase in the aggregation process.

The aggregation experiments were performed with recombinant Aβ(M1-40) peptide and showed that the influence of the cyclodextrins on the Aβ aggregation process depends on the cyclodextrin concentration but also on the

peptide concentration. The lag time of the aggregation was considerably shortened by increased peptide concentration. Concomitantly the effect of the cyclodextrins was decreased.

For all tested Aβ(M1-40) concentrations (3, 5, 8 and 15 μM), the β-cyclodextrin monomer in 0.1 and 1 mM concentration somewhat prolonged the lag time of the peptide aggregation. However, in 10 mM concentration it shortened the lag time, i.e. promoted aggregation. Moreover the β-cyclodextrin monomer in addition affected the amplitude of the ThT fluorescence. The higher the β-cyclodextrin monomer concentration, the stronger the amplitude reduction.

The α-cyclodextrin monomer had a similar, although weaker, influence on the lag time as the β-cyclodextrin monomer. However, concerning the amplitude the α-cyclodextrin monomer did not show any reducing effect. In contrast it rather seemed to somewhat increase the amplitude. It is interesting that the α- and β-cyclodextrin monomers differ in their influence on Aβ aggregation. This could be linked to the varying dimensions of the molecules.

In contrast to the lag time that is clearly connected to the peptide concentration (48), the amplitude of the ThT fluorescence curve is much more unpredictable and difficult to interpret. However, it is tempting to evaluate the amplitude in the presence of α- and β-cyclodextrin in terms of cyclodextrin binding affinity for the Aβ peptide, especially since earlier results have shown that there is no significant interaction between Aβ and the α-cyclodextrin monomer (149, 152). Perhaps the binding between the β-cyclodextrin monomer and Aβ(M1-40) is reflected in both the lag time and the amplitude and that the loss of amplitude reducing effect of the α-cyclodextrin monomer means a much weaker effect on the aggregation process.

The difference in amplitude caused by α- and β-cyclodextrin could also be due to that they may induce formation of different types of aggregates that have varying affinity for ThT. Another possibility could be that the β-cyclodextrin molecule in itself affects binding of ThT to the formed Aβ fibrillar aggregates.

The β-cyclodextrin dimer appeared to have a dual influence on the lag time. Dimer present at lower concentrations decreased the lag time of 3, 5 and 8 μM Aβ(M1-40) and hence accelerated aggregation. In contrast 10 mM β-cyclodextrin dimer increased the lag time of 5 and 8 μM peptide.

It is difficult to evaluate any ThT fluorescence amplitude effect of the β-cyclodextrin dimer. It seems like it in low concentrations somewhat increased the amplitude of the ThT fluorescence, especially at low peptide concentrations. At 3 and 8 μM Aβ(M1-40) the tendency is that 10 mM dimer reduced the amplitude.

It is interesting that the β-cyclodextrin dimer had an effect on Aβ aggregation that varied with both the peptide concentration and the dimer concentration. At low peptide concentration the dimer effects were more clearly distinguished than at high peptide concentrations. Possibly this can be explained by that the assembly process of Aβ monomers is slower at low peptide concentration and the dimer can more easily interfere with the aggregation. In a sample with a high concentration of Aβ peptides nuclei are quickly formed whose further assembly follows a fast and strong aggregation pathway that is difficult to affect.

The shortening of the Aβ lag time, especially seen at 3 μM peptide, in the presence of 0.5 and 5 mM dimer, could be a result of the dimer acting as a crosslinker. It might bind to two Aβ monomers that get in close contact, assemble and initiate the aggregation process. In contrast, when the β-cyclodextrin dimer is present in high concentration each peptide might be occupied by a dimer and the peptide-peptide contact is counteracted.

A dual effect on the Aβ aggregation has been observed also for amino modified polystyrene nanoparticles. It was seen that the ratio between Aβ peptide and particle concentration was crucial for the outcome of the aggregation and that a low particle surface area accelerated aggregation while a high particle surface area slowed down the aggregation (156).

In conclusion the various cyclodextrins were observed to interfere with the Aβ aggregation process and the outcome was seen to depend on the concentration of both peptide and cyclodextrin.

3.5 Paper V

pH dependence of the specific binding of Cu(II) and Zn(II) ions to the amyloid β peptide

In paper V the interaction of the metal ions Cu^{2+} and Zn^{2+} with Aβ(1-40) was studied by NMR and CD spectroscopy. Cu^{2+} and Zn^{2+} have been observed to be accumulated in amyloid plaques and to affect the aggregation of Aβ (22, 157).

The binding of Cu^{2+} to Aβ probably occurs as a mixture of two models; one of them involves D1 and the three histidines and the other involves the N-terminus, D1, H6, H13 and/or H14 (102). Zn^{2+} binds to all the histidines and D1 and possible also to for example E11 or H_2O (102). Obviously the two metal ions bind at least partly to the same ligands and this makes it possible for competition. The question of competition is interesting in the context of Alzheimer's disease since Cu^{2+} is redox active and connected to the formation of harmful ROS (158) while Zn^{2+} has been suggested to have a neuroprotective effect (159).

In the present study we investigated how the specific binding of Cu^{2+} and Zn^{+2} to Aβ(1-40) is influenced by various pHs. pH is an important factor that can be disturbed in the Alzheimer's disease brain due to inflammation (95).

Cu^{2+} and Zn^{2+} ions were titrated onto ^{15}N-labeled or $^{13}C,^{15}N$-labeled Aβ(1-40) at pHs 5.5, 6.5 and 7.4 and induced crosspeak intensity changes were followed by ^{1}H-^{15}N and ^{1}H-^{13}C HSQC spectra. It was found that at pH 7.4 both Cu^{2+} and Zn^{2+} caused a reduction of the amide crosspeak intensities of the Aβ N-terminal amino acid residues in the ^{1}H-^{15}N HSQC spectra. This is in general agreement with previous results (100) indicating specific binding of the metal ions to the nitrogen ligands on the histidines and to the N-terminus. In the case of Cu^{2+}, a possible linebroadening effect due to its paramagnetic properties could partly explain the crosspeak intensity reduction.

At pH 5.5 and 6.5 Cu^{2+} caused a pattern for crosspeak signal intensity reduction similar to the one at pH 7.4 in the ^{1}H-^{15}N HSQC spectra. However, the intensity in general, for the complete peptide sequence, was decreased. Probably this has to do with an increased Aβ aggregation at lower pH values.

In contrast to Cu^{2+}, Zn^{2+} did not cause the apparent N-terminal signal intensity reduction at pH 6.5. The effect was even smaller at pH 5.5, which could be due to that Zn^{2+} had lost or changed its specific binding for the peptide. Although this behavior may partly be due to a varying kinetic regime the observation suggests that the two ions do not compete for the same specific binding site at low pH.

The CD measurements show that Cu^{2+} induced a β-sheet state from the initial random coil conformation of Aβ(1-40). The aggregation was initiated at lower metal concentrations at pH 5.5 in comparison to pH 7.4. Zn^{2+} was incapable of inducing an Aβ state dominated by β-sheet structure at pH 7.4, the pH had to be decreased to 5.5 for this to happen.

In summary it seems like Cu^{2+} keeps its specific binding for Aβ at decreasing pH while Zn^{2+} shows a changed behavior. Hypothetically this could be of importance in the Alzheimer's disease brain where the pH can be decreased due to inflammation (95). At pH 7.4 the ions compete for the same ligands in the peptide, but at lower pH the competition from Zn^{2+} seems to be different and Cu^{2+} could get higher access to Aβ. This could worsen the conditions in the brain due to formation of ROS.

4. Future perspectives

My work during these years has added some new pieces to the jigsaw puzzle on the Aβ peptide, although a number of new questions has emerged along with the results. It would, for example, be very interesting to find out the size/sizes of the proposed β-sheet aggregates that are induced by detergent and CR. Further, how is the peptide organized in these assemblies? Another question is whether the peptide β-sheet structure in the presence of detergent, CR and β-cyclodextrin dimer is the same or different. Does the peptide adopt a β-hairpin conformation like in the presence of the Affibody dimer?

The toxicity of the β-sheet structures induced by the various molecules and metal ions should be investigated. Even though β-sheet structure is observed it could be of another character than in the oligomers reported to be neurotoxic (65). The formed assemblies could be modified in size, organization or surface, making them less toxic or even harmless. This has earlier been reported for CR; although it accelerates Aβ aggregation (145), it reduces the peptide toxicity (66, 143).

Even though the Aβ aggregation pathway can be quite well followed and characterized by various biophysical methods today, there are still several missing parts until the molecular disease mechanism(s) of Alzheimer's disease is (are) resolved.

5. Sammanfattning på svenska

Alzheimers sjukdom är en demenssjukdom som leder till att nervcellerna i hjärnan dör. Patienten förlorar minnet och orienteringsförmågan, genomgår personlighetsförändringar och får med tiden allt svårare att klara sig själv. För närvarande finns inget botemedel och sjukdomen leder till döden.

I hjärnan hos alzheimersjuka ser man ofta så kallade amyloida plack. I dessa plack, eller klumpar, hittar man en liten proteinbit som kallas amyloid beta (Aβ)-peptiden. Aβ-peptiden är både hydrofil och hydrofob och har en förmåga att aggregera (klistra ihop sig) med andra Aβ-peptider. I samband med aggregationen tappar peptiden sin ursprungliga, tämligen ostrukturerade form, och antar istället β-struktur. β-struktur innebär att peptiden veckar sig och flera sådana peptider bildar ett β-flak.

Från början trodde man att placken orsakar nervcellsdöden, men numera är uppfattningen att det är lösliga oligomera former av Aβ-peptiden som är den egentliga orsaken. Oligomerer är en samling av ett varierande antal, två till tolv eller betydligt många fler, aggregerade Aβ-peptider som troligen har antagit β-struktur.

I min avhandling har jag studerat Aβ-peptiden, hur den växelverkar med andra molekyler och hur dessa molekyler påverkar peptidens konformation. Den huvudsakliga metod som jag har använt för att följa förloppen är kärnmagnetresonansspektroskopi (NMR, Nuclear Magnetic Resonance). NMR ger atomär information om proteiner och peptider i lösning, bl a om deras tredimensionella struktur, hur de rör sig, hur stora de är och deras interaktioner med andra molekyler.

Molekylerna som Aβ-peptiden har studerats tillsammans med är detergenterna SDS och LiDS, färgämnet Congo-rött, en affibodymolekyl, en cyklodextrindimer samt de tvåvärda metalljonerna koppar och zink.

SDS och LiDS är detergentmolekyler bestående av en hydrofil huvudgrupp kopplad till en hydrofob svans. Dessa bildar miceller i vatten då huvudgrupperna vänder sig mot vattenmolekylerna medan svansarna göms inuti för att undvika kontakt med vattnet. Detta system används för att efterlikna cellmembranet.

Congo-rött används för att upptäcka β-struktur medan affibodymolekylen är ett protein som fungerar ungefär som en liten antikropp. Cyklodextrin-dimeren består av två ihopkopplade cyklodextrinmolekyler och vardera cyklodextrinmolekylen är en cirkulär sammankoppling av ett antal socker-molekyler. Metalljonerna är intressanta då de finns i placken i hjärnan.

Vi har sett att alla dessa molekyler samt jonerna påverkar Aβ-peptidens konformation. Aβ-peptider som omges av allt fler detergentmolekyler ändrar sin form från att vara ostrukturerade till att anta β-struktur till att slutligen få inslag av α-helix. Vi tolkar resulten som att detergent i mindre mängder kan få Aβ-peptiden att bilda oligomerer. Med större mängd detergent bildas detergentmiceller som binder peptiden till sig varvid α-helixform framkallas.

När Congo-rött tillsätts peptiden börjar händelseförloppet på samma sätt som då detergent tillsätts; Aβ-peptiderna är från början ostrukturerade men antar sen β-struktur. Skillnaden är dock att Congo-rött inte kan få Aβ-peptiden att övergå i α-helixform.

Affibodymolekylen är ett litet protein som binder parvis till Aβ-peptiden. Nästan hela peptiden omsluts av affibodyparet och antar β-struktur. För att effektivisera produktionen av affibodyn undersökte vi om den kan förkortas i ena änden. Det visade sig fungera och affibodyparet band till och med starkare till Aβ-peptiden i sin kortare form.

Cyklodextrin används inom framställningen av vissa läkemedel samt i en del smink- och livsmedelsprodukter för att förbättra löslighet och/eller stabilitet. Det har visat sig att cyklodextrinmolekylen binder till Aβ-peptiden och att den kan förhindra att peptiden aggregerar. Vi undersökte om cyklodextrin binder bättre till peptiden om cyklodextrinerna kopplas ihop två och två. Vi kunde se att denna dimer av cyklodextrin binder lite starkare till Aβ-peptiden än vad monomeren gör, och att både monomer och dimer form av cyklodextrin påverkar förloppet då peptiden aggregerar.

Slutligen studerade vi hur Aβ-peptiden påverkas av koppar- och zinkjoner vid ett allt lägre pH. Vid pH 7.4, dvs fysiologiskt pH, binder både koppar- och zinkjoner specifikt till peptidens tre histidiner och dess N-terminal vilket ger upphov till en tävlan mellan jonerna om bindning. Däremot, vid pH 5.5 fann vi att zinkjonerna ändrade sin specifika bindning till peptiden, medan kopparjonerna behöll den. Detta kan vara av betydelse i hjärnan hos en alzheimersjuk då miljön kan vara sur pga inflammation. Om tävlan förändras mellan zink- och kopparjonerna och kopparjoner i högre grad kan binda till peptiden kan flera skadliga ämnen bildas i reaktion med syre.

Sammanfattningsvis visar resultaten att Aβ-peptidens konformation och dess benägenhet att aggregera lätt påverkas av omgivningen. Denna anpassningsbarhet hos peptiden kan göra det lättare för den att anta en felaktig form, förslagsvis β-struktur, vilket i slutänden kan leda till utveckling av Alzheimers sjukdom.

6. Tack!

Stort tack **Astrid** för att du är en så himla bra handledare! Din entusiasm och glädje för forskning är smittande och det har varit väldigt roligt och inspirerande att få ta del av det. Du är mycket bra på att se det positiva i saker och ting, är en fenomenal problemlösare och jag har sedan i våras redan börjat sakna att sitta på ditt kontor och diskutera med dig.

Torbjörn, jag kan inte tacka dig nog för din omtänksamhet och hjälpsamhet under mina år på Biofysik. Du fixar ALLT, vad det än gäller, och du är ett suveränt fika- och lunchsällskap!

Haidi, tack för all hjälp med papper och intyg och allt annat som är värt att veta! Jag uppskattar även allt småprat, din omtänksamhet och dina positiva kommentarer.

Jüri, tack för att du lärde mig NMR, hur Aβ ska hanteras och för alla diskussioner och goda tips!

Jens, din avhandling är vältummad och välstuderad. Jag har uppskattat att du har funnits i huset och bistått med NMR-hjälp, kloka kommentarer och uppmuntrande support!

Sebastian, tack för vårt samarbete under de senaste åren. Det har varit väldigt värdefullt att få diskutera experiment och resultat med dig.

Axel, jag är så glad för att du anslöt dig till Aβ-gruppen (bestående av mig) och tog del av mina projekt. Tack för att du läste min avhandling (kommentaren ”Det är roligt att läsa den!” glädjer mig fortfarande) och kom med goda förbättringsförslag. Jag kommer sakna våra diskussioner och glada fniss på kontoret.

Sara, tack för att jag fick komma till ditt labb och göra Aβ-aggregations-experiment samt för goda synpunkter.

Risto, tack för all hjälp under veckan som jag tillbringade hos er på labbet i Lund och för att du visade hur Aβ-aggregationsexperiment bäst ska utföras! Ditt glada humör och ”det-ordnar-sig”-inställning glömmer jag inte.

Coco, tack för att jag under ett halvår fick vara doktorand i din grupp och ta del av den spännande prionvärlden.

Kajsa, tack för att du gjorde mitt första halvår som doktorand så bra! Jag minns första gången vi träffades och jag blev helt fascinerad av din energi och ditt sätt att berätta om projekten; du är den mest idérika och entusiastiska doktoranden (numera postdoc) som jag någonsin har träffat och inget problem är för stort.

Hanna, tack för all hjälp på cellabb, goda råd och uppmuntran under min tid i priongruppen.

Alex, tack för samarbetet under mitt första projekt och värdefulla tips för att hantera Aβ.

Jesper, tack för din hjälpsamhet med NMR experiment och datorprogram och inte minst för gott sällskap på den tiden då helgjobb var mer regel än undantag.

Lena & Peter, tack för hjälp med NMR experiment och goda kommentarer.

Fatemeh, ända sen jag kom till Biofysik har vi hängt ihop och jag kommer verkligen sakna att inte träffa dig varje dag! Jag gillar så våra diskussioner (rörande forskning och allt annat man kan tänka sig!), dagliga fikapauser, promenader, din pepp och support!

Scarlett, tack för tiden som min goa rumskompis och medresenär ut i vida världen (vi skulle klara oss hur bra som helst var som helst – eller hur?!), spontana efter-jobbet-middagar och en massa bra snack!

Sofia, jag minns precis tiden då vi var nya doktorander. Jag var väldigt glad över att du var där och uppskattar att vi har följts åt under alla år. Tack för alla bra pratstunder, tiden då vi delade kontor (saknar att du flyttade ut!) och roliga saker utanför jobbet!

Johannes, vad vore Biofysik utan dina funderingar, skämt och roliga idéer? Du sprider god stämning av bästa sort. Tack för att jag äntligen har fått kläm på figurhantering, det har underlättat ett flertal gånger den här sommaren.

Ye, thanks for your cheerfulness and enthusiasm, you always make me happy!

Britt-Marie, tack för att du alltid har ställt upp med hjälp på labb och för trevliga pratstunder.

Tack till mitt **lindy-hopgäng (Johannes, Sofia & Axel)** för outsinlig talang, ofelbar taktkänsla och stämning på topp!

Maria & Malin, det är så roligt att träffa er, fika, snacka och analysera det ena efter det andra i timmar! Saker och ting kommer på plats och energi fylls på.

Linda & Sanna, vad skulle jag göra utan er egentligen? Ni är bäst på att få mig att släppa taget och bara vara. Jag tycker så mycket om att hänga med er

och det som är viktigt blir med ens kristallklart. Tack **Peter** och **Johan** för peppmiddagar, skratt och goda råd!

Mormor & Morfar, tack för er omsorg, positiva hejarop och för att jag vet att ni tänker på mig. Det är en favorit att åka till er och bli ompysslad och få ett härligt bad i havet!

Sofia, du är den goaste och klokaste person som jag vet, alltid nära mig (om än inte geografiskt) och du är bäst på att liva upp stämningen! Jag kunde inte ha en bättre syster och bästa kompis.

Marcus, du är lugnet och tryggheten själv och det sprider sig runt dig. Du har bra lösningar på allt som jag kan tänka mig och en björnkram på det så är allt fixat. Du är min idol brorsan!

Mamma & Pappa, tack för att jag vet att ni finns där för mig oavsett vad det gäller och oavsett vad som än händer. Tack för er obegränsade support och omtanke i massor!

Doris, jag önskar att du vore här. Jag saknar att sitta i ditt kök, äta småkakor och prata. Jag minns fortfarande, även om det är en evighet sedan, vad jag svarade på din fråga om vad jag ville göra i framtiden; ”Forska – tänk vad spännande!”

Gun, tack för allt.

7. References

1. Chiti, F., and Dobson, C. M. (2006) Protein misfolding, functional amyloid, and human disease, *Annu. Rev. Biochem. 75*, 333-366.

2. Aguzzi, A., and O'Connor, T. (2010) Protein aggregation diseases: pathogenicity and therapeutic perspectives, *Nat. Rev. Drug Discov. 9*, 237-248.

3. Fändrich, M. (2007) On the structural definition of amyloid fibrils and other polypeptide aggregates, *Cell. Mol. Life Sci. 64*, 2066-2078.

4. Murphy, R. M. (2002) Peptide aggregation in neurodegenerative disease, *Annu. Rev. Biomed. Eng. 4*, 155-174.

5. Serpell, L. C. (2000) Alzheimer's amyloid fibrils: structure and assembly, *Biochim. Biophys. Acta 1502*, 16-30.

6. Cipriani, G., Dolciotti, C., Picchi, L., and Bonuccelli, U. (2011) Alzheimer and his disease: a brief history, *Neurol. Sci. 32*, 275-279.

7. Small, D. H., Losic, D., Martin, L. L., Turner, B. J., Friedhuber, A., and Aguilar, M. I. (2004) Alzheimer's disease therapeutics: New approaches to an ageing problem, *IUBMB Life 56*, 203-208.

8. Alzheimer's Association. *Alzheimer's Disease*. http://www.alz.org/documents/FSADFacts.pdf, May 17, 2007.

9. Yaari, R., and Corey-Bloom, J. (2007) Alzheimer's Disease, *Semin. Neurol. 27*, 32-42.

10. Alzheimer's Association. *Alzheimer's disease.* http://www.alz.org/alzheimers_disease_publications_alz_basics.asp, January 25, 2011.

11. Goedert, M., and Spillantini, M. G. (2006) A Century of Alzheimer's Disease, *Science 314*, 777-780.

12. Alzheimers.nu. *Om Alzheimers sjukdom.* http://www.alzheimers.nu/default____12350.aspx, October 18, 2007.

13. Svenskt Demens Centrum. *Alzheimers sjukdom.* http://www.demenscentrum.se/Fakta-om-demens/Demenssjukdomarna/Alzheimers-sjukdom/, January 26, 2011.

14. Blennow, K., de Leon, M. J., and Zetterberg, H. (2006) Alzheimer's disease, *Lancet 368*, 387-403.

15. Selkoe, D. J. (1994) Cell biology of the amyloid β-protein precursor and the mechanism of Alzheimer's disease, *Annu. Rev. Cell Biol. 10*, 373-403.

16. Fiala, J. C. (2007) Mechanisms of amyloid plaque pathogenesis, *Acta Neuropathol. 114*, 551-571.

17. Duyckaerts, C., Delatour, B., and Potier, M. C. (2009) Classification and basic pathology of Alzheimer disease, *Acta Neuropathol. 118*, 5-36.

18. Castellani, R. J., Rolston, R. K., and Smith, M. A. (2010) Alzheimer Disease, *Dis. Mon. 56*, 484-546.

19. Lansbury, P. T. J. (1996) A Reductionist View of Alzheimer's Disease, *Acc. Chem. Res. 29*, 317-321.

20. Hardy, J. A., and Higgins, G. A. (1992) Alzheimer's disease: The amyloid cascade hypothesis, *Science 256*, 184-185.

21. Estrada, L. D., and Soto, C. (2007) Disrupting β-amyloid aggregation for Alzheimer disease treatment, *Curr. Top. Med. Chem. 7*, 115-126.

22. Lovell, M. A., Robertson, J. D., Teesdale, W. J., Campbell, J. L., and Markesbery, W. R. (1998) Copper, iron and zinc in Alzheimer's disease senile plaques, *J. Neurol. Sci. 158*, 47-52.

23. Kang, J., Lemaire, H. G., Unterbeck, A., Salbaum, J. M., Masters, C. L., Grzeschik, K. H., Multhaup, G., Beyreuther, K., and Müller-Hill, B. (1987) The precursor of Alzheimer's disease amyloid A4 protein resembles a cell-surface receptor, *Nature 325*, 733-736.

24. Reinhard, C., Hébert, S. S., and De Strooper, B. (2005) The amyloid-β precursor protein: integrating structure with biological function, *EMBO J. 24*, 3996-4006.

25. Abad, C., Martínez-Gil, L., Tamborero, S., and Mingarro, I. (2009) Membrane topology of gp41 and amyloid precursor protein: Interfering transmembrane interactions as potential targets for HIV and Alzheimer treatment, *Biochim. Biophys. Acta 1788*, 2132-2141.

26. Selkoe, D. J. (2001) Alzheimer's Disease: genes, proteins, and therapy, *Physiol. Rev. 81*, 741-766.

27. Selkoe, D. J., Podlisny, M. B., Joachim, C. L., Vickers, E. A., Lee, G., Fritz, L. C., and Oltersdorf, T. (1988) β-Amyloid precursor protein of Alzheimer disease occurs as 110- to 135-kilodalton membrane-associated proteins in neural and non-neural tissues, *Proc. Natl. Acad. Sci. USA 85*, 7341-7345.

28. Haass, C., Schlossmacher, M. G., Hung, A. Y., Vigo-Pelfrey, C., Mellon, A., Ostaszewski, B. L., Lieberburg, I., Koo, E. H., Schenk, D., Teplow, D. B., and Selkoe, D. J. (1992) Amyloid β-peptide is produced by cultured cells during normal metabolism, *Nature 359*, 322-325.

29. Seubert, P., Vigo-Pelfrey, C., Esch, F., Lee, M., Dovey, H., Davis, D., Sinha, S., Schlossmacher, M., Whaley, J., Swindlehurst, C., McCormack, R., Wolfert, R., Selkoe, D., Lieberburg, I., and Schenk, D. (1992) Isolation and quantification of soluble Alzheimer's β-peptide from biological fluids, *Nature 359*, 325-327.

30. Mehta, P. D., Pirttilä, T., Mehta, S. P., Sersen, E. A., Aisen, P. S., and Wisniewski, H. M. (2000) Plasma and cerebrospinal fluid levels of amyloid β proteins 1-40 and 1-42 in Alzheimer disease, *Arch. Neurol. 57*, 100-105.

31. Haass, C., Hung, A. Y., Schlossmacher, M. G., Teplow, D. B., and Selkoe, D. J. (1993) β-Amyloid peptide and a 3-kDa fragment are derived by distinct cellular mechanisms, *J. Biol. Chem. 5*, 3021-3024.

32. Lazo, N. D., Maji, S. K., Fradinger, E. A., Bitan, G., and Teplow, D. B. (2005) The Amyloid β-Protein, in *Amyloid Proteins. The Beta Sheet Conformation and Disease*, 385-491, Wiley-VCH Verlag GmbH & Co, Weinheim, Germany.

33. Chow, V. W., Mattson, M. P., Wong, P. C., and Gleichmann, M. (2010) An overview of APP processing enzymes and products, *Neuromol. Med. 12*, 1-12.

34. Steiner, H., Fluhrer, R., and Haass, C. (2008) Intramembrane proteolysis by γ-secretase, *J. Biol. Chem. 283*, 29627-29631.

35. Mori, H., Takio, K., Ogawara, M., and Selkoe, D. J. (1992) Mass spectrometry of purified amyloid β protein in Alzheimer's disease, *J. Biol. Chem. 267*, 17082-17086.

36. Suzuki, N., Cheung, T. T., Cai, X. D., Odaka, A., Otvos, L., Eckman, C., Golde, T. E., and Younkin, S. G. (1994) An increased percentage of long amyloid β protein secreted by familial amyloid β protein precursor (βAPP_{717}) mutants, *Science 264*, 1336-1340.

37. Iwatsubo, T., Odaka, A., Suzuki, N., Mizusawa, H., Nukina, N., and Ihara, Y. (1994) Visualization of Aβ42(43) and Aβ40 in senile plaques with end-specific Aβ monoclonals: Evidence that an initially deposited species is Aβ42(43), *Neuron 13*, 45-53.

38. Gravina, S. A., Ho, L., Eckman, C. B., Long, K. E., Otvos, L., Younkin, L. H., Suzuki, N., and Younkin, S. G. (1995) Amyloid β protein (Aβ) in Alzheimer's disease brain, *J. Biol. Chem. 270*, 7013-7016.

39. Hou, L., Shao, H., Zhang, Y., Li, H., Menon, N. K., Neuhaus, E. B., Brewer, J. M., Byeon, I. J. L., Ray, D. G., Vitek, M. P., Iwashita, T., Makula, R. A., Przybyla, A. B., and Zagorski, M. G. (2004) Solution NMR studies of the Aβ(1-40) and Aβ(1-42) peptides establish that the Met35 oxidation state affects the mechanism of amyloid formation, *J. Am. Chem. Soc. 126*, 1992-2005.

40. Jarrett, J. T., Berger, E. P., and Lansbury, P. T. J. (1993) The carboxy terminus of the β amyloid protein is critical for the seeding of amyloid formation: implications for the pathogenesis of Alzheimer's disease, *Biochemistry 32*, 4693-4697.

41. Bush, A. I., Multhaup, G., Moir, R. D., Williamson, T. G., Small, D. H., Rumble, B., Pollwein, P., Beyreuther, K., and Masters, C. L. (1993) A Novel Zinc(II) Binding Site Modulates the Function of the βA4 Amyloid Protein Precursor of Alzheimer's Disease, *J. Biol. Chem. 268*, 16109-16112.

42. Hesse, L., Beher, D., Masters, C. L., and Multhaup, G. (1994) The βA4 amyloid precursor protein binding to copper, *FEBS Lett. 349*, 109-116.

43. Hardy, J., and Selkoe, D. J. (2002) The amyloid hypothesis of Alzheimer's disease: progress and problems on the road to therapeutics, *Science 297*, 353-356.

44. Armstrong, R. A. (2011) The pathogenesis of Alzheimer's disease: a reevaluation of the "amyloid cascade hypothesis", *Int. J. Alzheimers Dis. 7*, 1-6.

45. Montalto, M. C., Farrar, G., and Hehir, C. T. (2007) Fibrillar and oligomeric β-amyloid as distinct local biomarkers for Alzheimer's disease, *Ann. N. Y. Acad. Sci. 1097*, 239-258.

46. Harper, J. D., and Lansbury, P. T. J. (1997) Models of amyloid seeding in Alzheimer's disease and scrapie: Mechanistic truths and physiological consequences of the time-dependent solubility of amyloid proteins, *Annu. Rev. Biochem. 66*, 385-407.

47. Knowles, T. P. J., Waudby, C. A., Devlin, G. L., Cohen, S. I. A., Aguzzi, A., Vendruscolo, M., Terentjev, E. M., Welland, M. E., and Dobson, C. M. (2009) An analytical solution to the kinetics of breakable filament assembly, *Science 326*, 1533-1537.

48. Hellstrand, E., Boland, B., Walsh, D. M., and Linse, S. (2010) Amyloid β-protein aggregation produces highly reproducible kinetic data and occurs by a two-phase process, *ACS Chem. Neurosci. 1*, 13-18.

49. McLaurin, J., Yang, D. S., Yip, C. M., and Fraser, P. E. (2000) Review: Modulating factors in amyloid-β fibril formation, *J. Struct. Biol. 130*, 259-270.

50. Marcinowski, K. J., Shao, H., Clancy, E. L., and Zagorski, M. G. (1998) Solution structure model of residues 1-28 of the amyloid β-peptide when bound to micelles, *J. Am. Chem. Soc. 120*, 11082-11091.

51. Westermark, P., Benson, M. D., Buxbaum, J. N., Cohen, A. S., Frangione, B., Ikeda, S. I., Masters, C. L., Merlini, G., Saraiva, M. J., and Sipe, J. D. (2005) Amyloid: Toward terminology clarification. Report from the Nomenclature Committe of the International Society of Amyloidosis, *Amyloid 12*, 1-4.

52. Nelson, R., Sawaya, M. R., Balbirnie, M., Madsen, A. Ø., Riekel, C., Grothe, R., and Eisenberg, D. (2005) Structure of the cross-β spine of amyloid-like fibrils, *Nature 435*, 773-778.

53. Howie, A. J., and Brewer, D. B. (2009) Optical properties of amyloid stained by Congo red: History and mechanisms, *Micron 40*, 285-301.

54. Frid, P., Anisimov, S. V., and Popovic, N. (2007) Congo red and protein aggregation in neurodegenerative diseases, *Brain. Res. Rev. 53*, 135-160.

55. Klunk, W. E., Pettegrew, J. W., and Abraham, D. J. (1989) Quantitative evaluation of Congo red binding to amyloid-like proteins with a beta-pleated sheet conformation, *J. Histochem. Cytochem. 37*, 1273-1281.

56. Turnell, W. G., and Finch, J. T. (1992) Binding of the dye Congo red to the amyloid protein pig insulin reveals a novel homology amongst amyloid-forming peptide sequences, *J. Mol. Biol. 227*, 1205-1223.

57. Stopa, B., Piekarska, B., Konieczny, L., Rybarska, J., Spólnik, P., Zemanek, G., Roterman, I., and Król, M. (2003) The structure and protein binding of amyloid-specific dye reagents, *Acta Biochim. Pol. 50*, 1213-1227.

58. Khurana, R., Coleman, C., Ionescu-Zanetti, C., Carter, S. A., Krishna, V., Grover, R. K., Roy, R., and Singh, S. (2005) Mechanism of thioflavin T binding to amyloid fibrils, *J. Struct. Biol. 151*, 229-238.

59. LeVine III, H. (1993) Thioflavine T interaction with synthetic Alzheimer's disease β-amyloid peptides: Detection of amyloid aggegation in solution, *Protein Sci. 2*, 404-410.

60. Hawe, A., Sutter, M., and Jiskoot, W. (2008) Extrinsic fluorescent dyes as tools for protein characterization, *Pharm. Res. 25*, 1487-1499.

61. Biancalana, M., and Koide, S. (2010) Molecular mechanism of Thioflavin-T binding to amyloid fibrils, *Biochim. Biophys. Acta 1804*, 1405-1412.

62. Krebs, M. R. H., Bromley, E. H. C., and Donald, A. M. (2005) The binding of thioflavin-T to amyloid fibrils: Localisation and implications, *J. Struct. Biol. 149*, 30-37.

63. Voropai, E. S., Samtsov, M. P., Kaplevskii, K. N., Maskevich, A. A., Stepuro, V. I., Povarova, O. I., Kuznetsova, I. M., Turoverov, K. K., Fink, A. L., and Uverskii, V. N. (2003) Spectral properties of Thioflavin T and its complexes with amyloid fibrils, *J. Appl. Spectrosc. 70*, 868-874.

64. Groenning, M., Olsen, L., van de Weert, M., Flink, J. M., Frokjaer, S., and Jørgensen, F. S. (2007) Study in the binding of Thioflavin T to β-sheet-rich and non-β-sheet cavities, *J. Struct. Biol. 158*, 358-369.

65. Walsh, D. M., and Selkoe, D. J. (2007) Aβ Oligomers - a decade of discovery, *J. Neurochem. 101*, 1172-1184.

66. Lorenzo, A., and Yankner, B. A. (1994) β-Amyloid neurotoxicity requires fibril formation and is inhibited by Congo red, *Proc. Natl. Acad. Sci. USA 91*, 12243-12247.

67. Howlett, D. R., Jennings, K. H., Lee, D. C., Clark, M. S. G., Brown, F., Wetzel, R., Wood, S. J., Camilleri, P., and Roberts, G. W. (1995) Aggregation state and neurotoxic properties of Alzheimer beta-amyloid peptide, *Neurodegeneration 4*, 23-32.

68. Terry, R. D., Masliah, E., Salmon, D. P., Butters, N., DeTeresa, R., Hill, R., Hansen, L. A., and Katzman, R. (1991) Physical basis of cognitive alterations in Alzheimer's disease: Synapse loss is the major correlate of cognitive impairment, *Ann. Neurol. 30*, 572-580.

69. Lue, L. F., Kuo, Y. M., Roher, A. E., Brachova, L., Shen, Y., Sue, L., Beach, T., Kurth, J. H., Rydel, R. E., and Rogers, J. (1999) Soluble amyloid β peptide concentration as a predictor of synaptic change in Alzheimer's disease, *Am. J. Pathol. 155*, 853-862.

70. Dickson, D. W., Crystal, H. A., Mattiace, L. A., Masur, D. M., Blau, A. D., Davies, P., Yen, S. H., and Aronson, M. K. (1992) Identification of normal and pathological aging in prospectively studied nondemented elderly humans, *Neurobiol. Aging 13*, 179-189.

71. Hsia, A. Y., Masliah, E., McConlogue, L., Yu, G. Q., Tatsuno, G., Hu, K., Kholodenko, D., Malenka, R. C., Nicoll, R. A., and Mucke, L. (1999) Plaque-independent disruption of neural circuits in Alzheimer's disease mouse models, *Proc. Natl. Acad. Sci. USA 96*, 3228-3233.

72. McLean, C. A., Cherny, R. A., Fraser, F. W., Fuller, S. J., Smith, M. J., Beyreuther, K., Bush, A. I., and Masters, C. L. (1999) Soluble pool of Aβ amyloid as a determinant of severity of neurodegeneration in Alzheimer's disease, *Ann. Neurol. 46*, 860-866.

73. Kuo, Y. -., Emmerlings, M. R., Vigo-Pelfrey, C., Kasunic, T. C., Kirkpatrick, J. B., Murdoch, G. H., Ball, M. J., and Roher, A. E. (1996) Water-soluble Aβ (N-40, N-42) Oligomers in Normal and Alzheimer Disease Brains, *J. Biol. Chem. 271*, 4077-4081.

74. Lesné, S., Koh, M. T., Kotilinek, L., Kayed, R., Glabe, C. G., Yang, A., Gallagher, M., and Ashe, K. H. (2006) A specific amyloid-β protein assembly in the brain impairs memory, *Nature 440*, 352-357.

75. Podlisny, M. B., Ostaszewski, B. L., Squazzo, S. L., Koo, E. H., Rydell, R. E., Teplow, D. B., and Selkoe, D. J. (1995) Aggregation of secreted amyloid β-protein into sodium dodecyl sulfate-stable oligomers in cell culture, *J. Biol. Chem. 270*, 9564-9570.

76. Haass, C., and Selkoe, D. J. (2007) Soluble protein oligomers in neurodegeneration: lessons from the Alzheimer's amyloid β-peptide, *Nat. Rev. Mol. Cell Biol. 8*, 101-112.

77. Walsh, D. M., Lomakin, A., Benedek, G. B., Condron, M. M., and Teplow, D. B. (1997) Amyloid β-protein fibrillogenesis. Detection of a protofibrillar intermediate, *J. Biol. Chem. 272*, 22364-22372.

78. Lashuel, H. A., Hartley, D., Petre, B. M., Walz, T., and Lansbury, P. T. J. (2002) Neurodegenerative disease: amyloid pores from pathogenic mutations, *Nature 418*, 291.

79. Lambert, M. P., Barlow, A. K., Chromy, B. A., Edwards, C., Freed, R., Liosatos, M., Morgan, T. E., Rozovsky, I., Trommer, B., Viola, K. L., Wals, P., Zhang, C., Finch, C. E., Krafft, G. A., and Klein, W. L. (1998) Diffusible, nonfibrillar ligands derived from $A\beta_{1-42}$ are potent central nervous systems neurotoxins, *Proc. Natl. Acad. Sci. USA 95*, 6448-6453.

80. Walsh, D. M., Klyubin, I., Fadeeva, J. V., Cullen, W. K., Anwyl, R., Wolfe, M. S., Rowan, M. J., and Selkoe, D. J. (2002) Naturally secreted oligomers of amyloid β protein potently inhibit hippocampal long-term potentiation *in vivo*, *Nature 416*, 535-539.

81. Danielsson, J., Jarvet, J. D., P., and Gräslund, A. (2002) Translational diffusion measured by PFG-NMR on full length and fragments of the Alzheimer Aβ(1-40) peptide. Determination of hydrodynamic radii of random coil peptides of varying length, *Magn. Reson. Chem. 40*, S89-S97.

82. Danielsson, J., Jarvet, J., Damberg, P., and Gräslund, A. (2005) The Alzheimer β-peptide shows temperature-dependent transitions between left-handed 3_1-helix, β-strand and random coil secondary structures, *FEBS J. 272*, 3938-3949.

83. Rangachari, V., Reed, D. K., Moore, B. D., and Rosenberry, T. L. (2006) Secondary structure and interfacial aggregation of amyloid-β(1-40) on sodium dodecyl sulfate micelles, *Biochemistry 45*, 8639-8648.

84. Tew, D. J., Bottomley, S. P., Smith, D. P., Ciccotosto, G. D., Babon, J., Hinds, M. G., Masters, C. L., Cappai, R., and Barnham, K. J. (2008) Stabilization of neurotoxic soluble β-sheet-rich conformations of the Alzheimer's disease amyloid-β peptide, *Biophys. J. 94*, 2752-2766.

85. Coles, M., Bicknell, W., Watson, A. A., Fairlie, D. P., and Craik, D. J. (1998) Solution structure of amyloid β-peptide(1-40) in a water-micelle environment. Is the membrane-spanning domain where we think it is? *Biochemistry 37*, 11064-11077.

86. Shao, H., Jao, S., Ma, K., and Zagorski, M. G. (1999) Solution structures of micelle-bound amyloid β-(1-40) and β-(1-42) peptides of Alzheimer's disease, *J. Mol. Biol. 285*, 755-773.

87. Jarvet, J., Danielsson, J., Damberg, P., Oleszczuk, M., and Gräslund, A. (2007) Positioning of the Alzheimer Aβ(1-40) peptide in SDS micelles using NMR and paramagnetic probes, *J. Biomol. NMR 39*, 63-72.

88. Pervushin, K., Riek, R., Wider, G., and Wütrich, K. (1997) Attenuated T_2 relaxation by mutual cancellation of dipole-dipole coupling and chemical shift anisotropy indicates an avenue to NMR structures of very large biological macromolecules in solution, *Proc. Natl. Acad. Sci. USA 94*, 12366-12371.

89. Hoyer, W., Grönwall, C., Jonsson, A., Ståhl, S., and Härd, T. (2008) Stabilization of a β-hairpin in monomeric Alzheimer's amyloid-β peptide inhibits amyloid formation, *Proc. Natl. Acad. Sci. U. S. A. 105*, 5099-5104.

90. Lendel, C., Wahlberg, E., Berglund, H., Eklund, M., Nygren, P. Å., and Härd, T. (2002) ^{1}H, ^{13}C and ^{15}N resonance assignments of an affibody-target complex, *J. Biomol. NMR 24*, 271-272.

91. Grönwall, C., Jonsson, A., Lindström, S., Gunneriusson, E., Ståhl, S., and Herne, N. (2007) Selection and characterization of Affibody ligands binding to Alzheimer amyloid β peptides, *J. Biotechnol. 128*, 162-183.

92. Adlard, P. A., and Bush, A. I. (2006) Metals and Alzheimer's disease, *J. Alzheimers Dis. 10*, 145-163.

93. Hung, Y. H., Bush, A. I., and Cherny, R. A. (2010) Copper in the brain and Alzheimer's disease, *J. Biol. Inorg. Chem. 15*, 61-76.

94. Frederickson, C. J., Koh, J. Y., and Bush, A. I. (2005) The neurobiology of zinc in health and disease, *Nat. Rev. Neurosci. 6*, 449-462.

95. Atwood, C. S., Moir, R. D., Huang, X., Scarpa, R. C., Bacarra, N. M. E., Romano, D. M., Hartshorn, M. A., Tanzi, R. E., and Bush, A. I. (1998) Dramatic aggregation of Alzheimer Aβ by Cu(II) is induced by conditions representing physiological acidosis, *J. Biol. Chem. 273*, 12817-12826.

96. Garai, K., Sengupta, P., Sahoo, B., and Maiti, S. (2006) Selective destabilization of soluble amyloid β oligomers by divalent metal ions, *Biochem. Biophys. Res. Commun. 345*, 210-215.

97. Sarell, C. J., Wilkinson, S. R., and Viles, J. H. (2010) Substoichiometric levels of Cu^{2+} ions accelerate the kinetics of fiber formation and promote cell toxicity of amyloid-β from Alzheimer Disease, *J. Biol. Chem. 285*, 41533-41540.

98. Yoshiike, Y., Tanemura, K., Murayama, O., Akagi, T., Murayama, M., Sato, S., Sun, X., Tanaka, N., and Takashima, A. (2001) New insights on how metals disrupt amyloid β-aggregation and their effects on amyloid-β cytotoxicity, *J. Biol. Chem. 276*, 32293-32299.

99. Syme, C. D., and Viles, J. H. (2006) Solution ^{1}H NMR investigation of Zn^{2+} and Cd^{2+} binding to amyloid-beta peptide (Aβ) of Alzheimer's disease, *Biochim. Biophys. Acta 1764*, 246-256.

100. Danielsson, J., Pierattelli, R., Banci, L., and Gräslund, A. (2007) High-resolution NMR studies of the zinc-binding site of the Alzheimer's amyloid β-peptide, *FEBS J. 274*, 46-59.

101. Hou, L., and Zagorski, M. G. (2006) NMR reveals anomalous copper(II) binding to the amyloid Aβ peptide of Alzheimer's disease, *J. Am. Chem. Soc. 128*, 9260-9261.

102. Faller, P., and Hureau, C. (2009) Bioinorganic chemistry of copper and zinc ions coordinated to amyloid-β peptide, *Dalton Trans.* , 1080-1094.

103. Amijee, H., and Scopes, D. I. C. (2009) The quest for small molecules as amyloid inhibiting therapies for Alzheimer's disease, *J. Alzheimers Dis. 17*, 33-47.

104. Necula, M., Kayed, R., Milton, S., and Glabe, C. G. (2007) Small molecule inhibitors of aggregation indicate that amyloid β oligomerization and fibrillization pathways are independent and distinct, *J. Biol. Chem. 282*, 10311-10324.

105. Ladiwala, A. R. A., Dordick, J. S., and Tessier, P. M. (2011) Aromatic small molecules remodel toxic soluble oligomers of amyloid β through three independent pathways, *J. Biol. Chem. 286*, 3209-3218.

106. Purcell, E. M., Torrey, H. C., and Pound, R. V. (1946) Resonance absorption by nuclear magnetic moments in a solid, *Phys. Rev. 69*, 37-38.

107. Bloch, F., Hansen, W. W., and Packard, M. (1946) Nuclear induction, *Phys. Rev. 69*, 127.

108. Keeler, J. (2006) *Understanding NMR Spectroscopy.* 1st ed, 5-80, 194-195, 214-215, 226-227, 286-287, 357. John Wiley & Sons Ltd, Chichester, West Sussex, England.

109. Levitt, M. H. (2008) *Spin Dynamics - Basics of Nuclear Magnetic Resonance.* 2nd ed, 5-118. John Wiley & Sons Ltd, Chichester, West Sussex, England.

110. Aue, W. P., Bartholdi, E., and Ernst, R. R. (1976) Two-dimensional spectroscopy. Applications to nuclear magnetic resonance, *J. Chem. Phys. 64*, 2229-2246.

111. Braunschweiler, L., and Ernst, R. R. (1983) Coherence transfer by isotropic mixing: Application to proton correlation spectroscopy, *J. Magn. Reson. 53*, 521-528.

112. Jeener, J., Meier, B. H., Bachmann, P., and Ernst, R. R. (1979) Investigation of exchange processes by two-dimensional NMR spectroscopy, *J. Chem. Phys. 71*, 4546-4553.

113. Bodenhausen, G., and Ruben, D. J. (1980) Natural abundance nitrogen-15 NMR by enhanced heteronuclear spectroscopy, *Chem. Phys. Lett. 69*, 185-189.

114. Bain, A. D. (1998) Blurring the distinction between slow and intermediate chemical exchange, *Biochem. Cell. Biol. 76*, 171-176.

115. Kanelis, V., Forman-Kay, J. D., and Kay, L. E. (2001) Multidimensional NMR methods for protein structure determination, *IUBMB Life 52*, 291-302.

116. Sattler, M., Schleucher, J., and Griesinger, C. (1999) Heteronuclear multidimensional NMR experiments for the structure determination of proteins in solution employing pulsed field gradients, *Prog. Nucl. Magn. Reson. Spectrosc. 34*, 93-158.

117. Price, W. S. (1997) Pulsed-field gradient nuclear magnetic resonance as a tool for studying translational diffusion: Part 1. Basic theory, *Magnetic Resonance: an Educational Journal 9*, 299-336.

118. Nicolay, K., Braun, K. P. J., de Graaf, R. A., Dijkhuizen, R. M., and Kruiskamp, M. J. (2001) Diffusion NMR spectroscopy, *NMR Biomed. 14*, 94-111.

119. Stejskal, E. O., and Tanner, J. E. (1965) Spin diffusion measurements: Spin echoes in the presence of a time-dependent field gradient, *J. Chem. Phys. 42*, 288-292.

120. Hrabe, J., Kaur, G., and Guilfoyle, D. N. (2007) Principles and limitations of NMR diffusion measurements, *J. Med. Phys. 32*, 34-42.

121. Fasman, G. D. (1996) *Circular Dichroism and the Conformational Analysis of Biomolecules*, 1st ed, 635-652. Plenum Press, New York, USA.

122. Marshall, A. G. (1978) *Biophysical Chemistry - Principles, Techniques and Applications*, 1st ed, 364-367. John Wiley & Sons Inc, USA.

123. Berova, N., Nakanishi, K., and Woody, R. W. (2000) *Circular Dichroism - Principles and Applications*, 2nd ed, 1-35, 55-95, 601-620. Wiley-VCH Inc, New York, USA.

124. Greenfield, N. J. (1996) Methods to estimate the conformation of proteins and polypeptides from circular dichroism data, *Anal. Biochem. 235*, 1-10.

125. Greenfield, N., and Fasman, G. D. (1969) Computed circular dichroism spectra for the evaluation of protein conformation, *Biochemistry 8*, 4108-4116.

126. Jarvet, J. *Circular dichroism: standard spectra.* Personal communication November 1, 2007.

127. Lakowicz, J. R. (1999) *Principles of Fluorescence Spectroscopy*, 2nd ed, 1-23, 445-486. Kluwer Academic/Plenum Publishers, New York, USA.

128. Campbell, I. D., and Dwek, R. A. (1984) *Biological Spectroscopy*, 1st ed, 91-126. The Benjamin/Cummings Publishing Company Inc, Menlo Park, California, USA.

129. Henry, G. D., and Sykes, B. D. (1994) Methods to study membrane protein structure in solution, *Methods Enzymol. 239*, 515-535.

130. Damberg, P., Jarvet, J., and Gräslund, A. (2001) Micellar systems as solvents in peptide and protein structure determination, *Methods Enzymol. 339*, 271-285.

131. Marcotte, I., and Auger, M. (2005) Bicelles as model membranes for solid- and solution-state NMR studies of membrane peptides and proteins, *Concepts Magn. Reson. Part A 24A*, 17-37.

132. Whiles, J. A., Deems, R., Regitze, R. V., and Dennis, E. A. (2002) Bicelles in structure-function studies of membrane-associated proteins, *Bioorg. Chem. 30*, 431-442.

133. Garavito, R. M., and Ferguson-Miller, S. (2001) Detergents as tools in membrane biochemistry, *J. Biol. Chem. 276*, 32403-32406.

134. Otzen, D. E. (2010) Amyloid formation in surfactants and alcohols: Membrane mimetics or structural switchers? *Curr. Protein Pept. Sci. 11*, 355-371.

135. Kohno, T., Kobayashi, K., Maeda, T., Sato, K., and Takashima, A. (1996) Three-dimensional structures of the amyloid β peptide (25-35) in membrane-mimicking environment, *Biochemistry 35*, 16094-16104.

136. Mukerjee, P., Mysels, K. J., and Kapauan, P. (1967) Counterion specificity in the formation of ionic micelles - size, hydration, and hydrophobic bonding effects, *J. Phys. Chem. 71*, 4166-4175.

137. Lührs, T., Ritter, C., Adrian, M., Riek-Loher, D., Bohrmann, B., Döbeli, H., Schubert, D., and Riek, R. (2005) 3D structure of Alzheimer's amyloid-β(1-42) fibrils, *Proc. Natl. Acad. Sci. U. S. A. 102*, 17342-17347.

138. Rangachari, V., Reed, D. K., Moore, B. D., and Rosenberry, T. L. (2006) Secondary structure and interfacial aggregation of amyloid-β(1-40) on sodium dodecyl sulfate micelles, *Biochemistry 45*, 8639-8648.

139. Verdier, Y., Zarándi, M., and Penke, B. (2004) Amyloid β-peptide interactions with neuronal and glial cell plasma membrane: Binding sites and implications for Alzheimer's disease, *J. Peptide Sci. 10*, 229-248.

140. Schulman, B. A., Kim, P. S., Dobson, C. M., and Redfield, C. (1997) A residue-specific NMR view of the non-cooperative unfolding of a molten globule, *Nat. Struct. Biol. 4*, 630-634.

141. Kumar, S., Singh, A. K., Krishnamoorthy, G., and Swaminathan, R. (2008) Thioflavin T displays enhanced fluorescence selectively inside anionic micelles and mammalian cells, *J. Fluoresc. 18*, 1199-1205.

142. Tjernberg, L. O., Näslund, J., Lindqvist, F., Johansson, J., Karlström, A. R., Thyberg, J., Terenius, L., and Nordstedt, C. (1996) Arrest of β-amyloid fibril formation by a pentapeptide ligand, *J. Biol. Chem. 271*, 8545-8548.

143. Crowther, D. C., Kinghorn, K. J., Miranda, E., Page, R., Curry, J. A., Duthie, F. A. I., Gubb, D. C., and Lomas, D. A. (2005) Intraneuronal Aβ, non-amyloid aggregates and neurodegeneration in a *Drosophila* model of Alzheimer's disease, *Neuroscience 132*, 123-135.

144. Kim, Y. S., Randolph, T. W., Manning, M. C., Stevens, F. J., and Carpenter, J. F. (2003) Congo red populates partially unfolded states of an amyloidogenic protein to enhance aggregation and amyloid fibril formation, *J. Biol. Chem. 278*, 10842-10850.

145. Pedersen, M. Ø., Mikkelsen, K., Behrens, M. A., Pedersen, J. S., Enghild, J. J., Skrydstrup, T., Malmendal, A., and Nielsen, N. C. (2010) NMR reveals two-step association of Congo Red to amyloid β in low-molecular-weight aggregates, *J. Phys. Chem. B 114*, 16003-16010.

146. Bose, P. P., Chatterjee, U., Xie, L., Johansson, J., Göthelid, E., and Arvidsson, P. I. (2010) Effects of Congo Red on Aβ1-40 fibril formation process and morphology, *ACS Chem. Neurosci. 1*, 315-324.

147. Nord, K., Gunneriusson, E., Ringdahl, J., Ståhl, S., Uhlén, M., and Nygren, P. Å. (1997) Binding proteins selected from combinatorial libraries of an α-helical bacterial receptor domain, *Nat. Biotechnol. 15*, 772-777.

148. Hoyer, W., and Härd, T. (2008) Interaction of Alzheimer's Aβ peptide with an engineered binding protein - thermodynamics and kinetics of coupled folding-binding, *J. Mol. Biol. 378*, 398-411.

149. Danielsson, J., Jarvet, J., Damberg, P., and Gräslund, A. (2004) Two-site binding of β-cyclodextrin to the Alzheimer Aβ(1-40) peptide measured with combined PFG-NMR diffusion and induced chemical shifts, *Biochemistry 43*, 6261-6269.

150. Szejtli, J. (1998) Introduction and general overview of cyclodextrin chemistry, *Chem. Rev. 98*, 1743-1753.

151. Loftsson, T., and Duchêne, D. (2007) Cyclodextrins and their pharmaceutical applications, *Int. J. Pharm. 329*, 1-11.

152. Qin, X. R., Abe, H., and Nakanishi, H. (2002) NMR and CD studies on the interaction of Alzheimer β-amyloid peptide (12-28) with β-cyclodextrin, *Biochem. Biophys. Res. Commun. 297*, 1011-1015.

153. Camilleri, P., Haskins, N. J., and Howlett, D. R. (1994) β-Cyclodextrin interacts with the Alzheimer amyloid β-A4 peptide, *FEBS Lett. 341*, 256-258.

154. Waite, J., Cole, G. M., Frautschy, S. A., Connor, D. J., and Thal, L. J. (1992) Solvent effects on beta protein toxicity in vivo, *Neurobiol. Aging 13*, 595-599.

155. Wang, M. S., Boddapati, S., and Sierks, M. R. (2009) Cyclodextrins promote protein aggregation posing risks for therapeutic applications, *Biochem. Biophys. Res. Commun. 386*, 526-531.

156. Cabaleiro-Lago, C., Quinlan-Pluck, F., Lynch, I., Dawson, K. A., and Linse, S. (2010) Dual effect of amino modified polystyrene nanoparticles on amyloid β protein fibrillation, *ACS. Chem. Neurosci. 1*, 279-287.

157. Faller, P. (2009) Copper and zinc binding to amyloid-β: Coordination, dynamics, aggregation, reactivity and metal-ion transfer, *Chembiochem. 10*, 2837-2845.

158. Huang, X., Moir, R. D., Tanzi, R. E., Bush, A. I., and Rogers, J. T. (2004) Redox-active metals, oxidative stress, and Alzheimer's disease pathology, *Ann. N. Y. Acad. Sci. 1012*, 153-163.

159. Cuajungco, M. P., Goldstein, L. E., Nunomura, A., Smith, M. A., Lim, J. T., Atwood, C. S., Huang, X., Farrag, Y. W., Perry, G., and Bush, A. I. (2000) Evidence that the β-amyloid plaques of Alzheimer's disease represent the redox-silencing and entombment of Aβ by zinc, *J. Biol. Chem. 275*, 19439-19442.

160. Hölscher, C. (1999) Synaptic plasticity and learning and memory: LTP and beyond, *J. Neurosci. Res. 58*, 62-75.